Fuel Processing Technology 250 (2023) 107917

Contents lists available at ScienceDirect

Fuel Processing Technology

journal homepage: www.elsevier.com/locate/fuproc

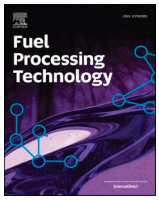

Analytical (hydro)pyrolysis of pinewood and wheat straw in chloride molten salts: A route for 2-methyl furan production

Adriana Estrada Leon [a,*], Racchana Ramamurthy [b], Stef Ghysels [a], Sepideh Niazi [c], Wolter Prins [a], Frederik Ronsse [a]

[a] Thermochemical Conversion of Biomass Research Group, Department of Green Chemistry and Technology, Ghent University, Coupure Links 653, B-9000, Belgium
[b] Department of Civil Engineering, McGill University, Montreal, Quebec H3A 0C3, Canada
[c] Faculty of science and technology, Norwegian University of Life Science (NMBU), Ås, Norway

ARTICLE INFO

Keywords:
Chloride molten salts
Hydropyrolysis.
Lignocellulosic biomass.
2-methyl furan.

ABSTRACT

2-methyl furan (MF) is a fuel additive with improved fuel characteristics compared to bio-ethanol. Unfortunately, the production of MF (from furfural (FF) hydrogenation) is not economically feasible. Interestingly, molten salts in biomass pyrolysis have shown to promote the formation of furans (mainly FF). Because molten salts hydropyrolysis could be an alternative route to both produce FF and convert it into MF, an assessment is indispensable. Molten salts pyrolysis and hydropyrolysis of pinewood and wheat straw and related model compounds were studied in a micro-reactor. The effect of hydropyrolysis process variables was assessed on the total detectable condensable vapors and MF formation.

At low pressures (0.4 MPa), the chloride salts favored the production of FF and acetic regardless of the reaction atmosphere. Under a high pressure of hydrogen though (1.6 and 3.0 MPa), the conversion of FF to MF was enhanced through hydrogenation, hydrodeoxygenation and demethylation reactions. Molten salts hydropyrolysis at 350 °C and pressures of either 1.6 MPa (biomass mass fraction of 0.09) or 3.0 MPa (biomass mass fraction of 0.24) were optimal and yielded ca. 8 wt% to 9 wt% MF. Reaction temperatures >350 °C were unfavorable for the MF yield and instead promoted furfural decarbonylation to furan.

1. Introduction

Within the transportation sector in the EU, the use of gasoline still remains crucial and accounts for 28.2% of the current fuel sales. It has been reported that 85% of that fraction of gasoline is a blend-fuel which contains bioethanol [1]. In 2016, 75% of the gasoline sold in the EU had up to 5% bio-ethanol by volume (E5 gasoline) and 10% had up to 10% bio-ethanol (E10 gasoline) by volume [1,2]. If the EU would adopt E20 gasoline (20% volume ethanol-petrol) by 2030, to further reduce the current CO_2 emissions from gasoline up to 8.2%, the demand for bio-ethanol is only expected to increase [3,4]. Recently, researchers have shown an increased interest in 2-methyl furan (MF) as a promising second generation biofuel that can be used in existing internal combustion engines (particularly in spark ignition engines). It has better fuel properties than bio-ethanol. Compared to bio-ethanol, MF is higher in energy density and has a lower latent heat of vaporization which can result in better fuel economy [5]. Moreover, MF has a higher research octane number (RON = 103) than that of gasoline (RON = 96.8) [6]. Within the possible reaction pathways to generate MF, catalytic hydrogenation of furfural (FF) either in the liquid-phase or vapor-phase stands out [5–7]. Fairly high conversion yields from FF to MF (> 90%) have already been achieved with Cu-based catalysts [8,9]. In spite of that, the main barrier in MF turnout is the economical aspect, which is centered around the significant cost that is imposed by the pretreatment of lignocellulosic biomasses, necessary to attain higher FF yields as intermediate platform [5]. In addition to the economical aspect, MF production from FF might not be straightforward because the main drawback of furan aldehydes such as FF is their instability during storage. This makes FF susceptible to polymerize to humins and also darken due to air oxidation [10]. From this point of view it is more reasonable to start from the stable biomass and to produce MF directly and in-situ from FF.

It has been demonstrated that molten salts pyrolysis of lignocellulosic biomass can be a prospective route to selectively produce furan-ring compounds [11,12]. Molten salts therefore have a role as a catalyst in pyrolysis, but also have a capacity as heat transfer medium and a

* Corresponding author.
E-mail address: Adriana.EstradaLeon@ugent.be (A. Estrada Leon).

https://doi.org/10.1016/j.fuproc.2023.107917
Received 3 April 2023; Received in revised form 13 June 2023; Accepted 3 July 2023
Available online 14 July 2023

reactive fluid [13]. Particularly, eutectic mixtures composed of chloride salts $ZnCl_2$, KCl and NaCl have shown high catalytic activity towards FF production during pyrolysis of biomass [12]. Molten salts have shown to improve the heat transfer of biomass particles compared to traditional fluidized sand beds at temperatures of approx. 500 °C [14,15]. This allows for the possibility to conduct molten salt pyrolysis at temperatures lower than 500 °C while maintaining similar or higher heat flux towards the biomass particles. Moreover, with eutectic mixtures of $ZnCl_2$, KCl and NaCl particularly, pyrolysis temperatures above 350 °C were deemed not suitable because these can volatilize and infiltrate downstream of the reactors [11].

Now, within thermochemical conversion technologies such as pyrolysis, the search to upgrade the quality of derived bio-liquids continues to attract attention and one considered choice is hydropyrolysis [16]. Hydropyrolysis, defined as the rapid thermal decomposition of an organic material under a H_2 atmosphere, produces hydrogen radicals that can react with the volatiles released, removing oxygen in the form of water, CO and CO_2, and producing hydrocarbons [16]. Wang et al. (2022) investigated the influence of reaction atmospheres (He vs. H_2) for pyrolysis in a micro-scale reactor at 3.0 MPa and 500 °C and found that H_2 changed significantly the product distribution from cellulose [17]. Mainly, it was observed that the H/C ratio of the condensable vapors obtained from cellulose hydropyrolysis increased from 1.4 to 1.9 when compared to cellulose pyrolysis, showing that H_2 effectively participated in the pyrolysis process, predominantly throughout the promotion of hydrogenation and hydrodeoxygenation (HDO) reactions [17]. Moreover, hydropyrolysis of lignin at 3.0 MPa and 500 °C has also demonstrated to be advantageous over conventional pyrolysis because it has boosted the conversion of methoxy phenolics to non-methoxy phenolics and facilitated the production of hydrocarbon condensable vapors and hydrocarbon gases [18,19]. Importantly, a higher H_2 pressure suggests higher concentration of hydrogen free radicals (formed by homolytic or heterolytic cleavage of the H—H bond) which leads to an increased rate of hydrogenation and HDO reactions [16]. Stummann et al. (2019) showed that in catalytic hydropyrolysis of beech wood, H_2 pressures >1.59 MPa prevented re-polymerization reactions from the volatiles which resulted in higher volatiles' yield in addition to the production of an oxygen-free condensed organic phase (oxygen <0.01 wt%) [20].

So far, no studies have investigated molten salts hydropyrolysis of lignocellulosic biomass as an alternative route to generate furan-ring compounds which can be converted in the vapor phase to MF. One of the purposes of this paper is to first compare quantitative micro-scale pyrolysis and hydropyrolysis of lignocellulosic biomass in chloride molten salts ($ZnCl_2$:KCl:NaCl) to elucidate the effect of the carrier gas used and the catalytic effect of the salts on both the volatiles yield and quality. To support this objective, model compounds from holocellulose and lignin-derived intermediates were first pyrolyzed under helium and hydrogen, and in the presence and absence of molten chloride salts, to comprehend the effect on the distribution of the volatile pyrolysis products. The second objective of this study was to determine optimal process conditions for molten salts hydropyrolysis of lignocellulosic biomass (in terms of pressure, biomass concentration and temperature) giving a good trade-off between the yield of pyrolysis vapors and their hydrogenation/hydrodeoxygenation rate. Thermal decomposition of lignocellulosic biomass with individual chloride salts ($ZnCl_2$, KCl, and NaCl) is also investigated, to explore which of the constituent salts in the molten salt eutectic mixture causes the catalytic reactions observed.

2. Materials and methods

2.1. Materials and sample preparation

The lignocellulosic feedstock materials used in this study were pinewood (Lignocel®) and wheat straw (supplied by Aston University). Prior their use, the feedstock were dried at 105 °C and sieved to a particle size <100 μm. The characteristics of these feedstock samples have been previously described in [11].

Zinc (II) chloride (> 98%, Sigma Aldrich), potassium chloride (> 98% Sigma Aldrich) and sodium chloride (> 99%, Sigma Aldrich) were used to prepare an eutectic mixture with a composition of 44.3–41.9-13.8 mol% respectively. The $ZnCl_2$:KCl:NaCl mixture used (named salt B in our previous study) has a melting point of 204 °C [21]. Salt B was selected because of its stability during pyrolysis and its performance as a catalytic reaction medium. For the preparation of salt B, the individual salts were heated individually to 300 °C for 24 h in porcelain crucibles. Upon cooling down to 105 °C, the dried salts were mixed in their corresponding molar concentration and then stored at 105 °C until further usage.

The samples were prepared in eco-cups (Rx-3050TR, Frontier Laboratories Ltd., 8 mm H x 4 mm O.D.) made of deactivated stainless steel. The eco-cups were placed in eco-stands to hold them in position during weighing the lignocellulosic feedstock and salts. The weight of the feedstock sample measured for the micro-scale experiments was ca. 250–300 μg using a Mettler Toledo XP6 Microbalance (1 μg precision). Depending on the experiment, the required amount of salt B was measured and added to the eco-cup. The contents of then eco-cup were then mixed by hand using an eco-stick (Rx-3050TR, Frontier Laboratories Ltd., L 80 mm). A small amount of quartz wool was placed on top of the sample into the eco-cup to prevent the escape of the salts and feedstock during the pyrolysis experiment as it can lead to the contamination of the TMR. Finally, an eco-stick for single shot analysis (Rx-3050TR, Frontier Laboratories Ltd., 30 mm L) was inserted into the eco-cup to put the contents of the cup in place.

2.2. Micro-reactor configuration (py-GC-MS/FID)

Micro-pyrolysis experiments were performed in a high pressure tandem micro reactor (Rx-3050TR, Frontier Laboratories Ltd.) with two carrier gases individually: helium (Air Products, 99.9999% purity) and hydrogen (Air Liquide, 99.9999% purity). The tandem micro reactor (TMR) was coupled to a gas chromatograph (Thermo Fisher Scientific Trace GC Ultra), a mass spectrometer (Thermo ISQ MS) and a flame ionization detector (FID). Fig. 1 shows a scheme of the py-GC–MS/FID system used. The carrier gas employed in the system was controlled by a high pressure flow controller (HP-3050F, Frontier Laboratories Ltd). The controller was used to set the pressure in the TMR (named BP1), and also to establish the GC column inlet pressure (named BP2) which controlled the column flow. The pressures used in the TMR ranged from 0.4 MPa to 3.0 MPa. A high pressure solid sampler was used to introduce stainless-steel cups (4 mm internal diameter and 8 mm height, Frontier

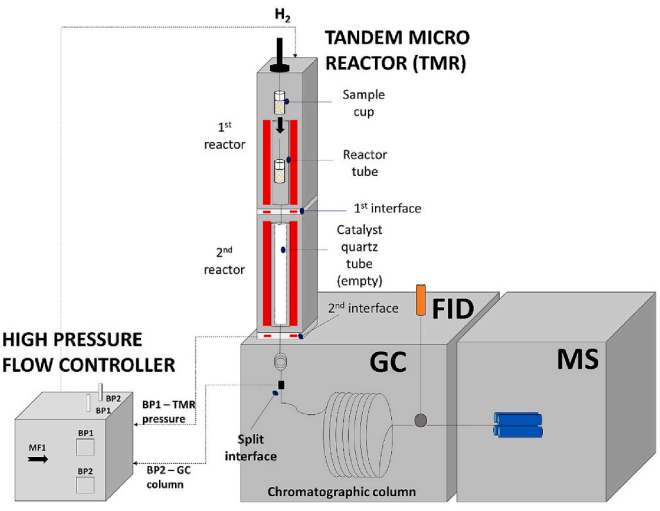

Fig. 1. Scheme of the py-GC–MS/FID system used for molten salts micropyrolysis.

Laboratories Ltd.) containing the solid samples or calibration mixtures. In this study, only the first reactor was utilized to pyrolyze solid samples (or calibrate the TMR), while the second reactor remained empty. During micro-pyrolysis experiments, the temperature of the second interface was kept constant at 280 °C, similar to the inlet temperature of the GC column. The temperature of the first interface and the second reactor were kept at 320 °C.

To maintain a stable carrier gas flow rate in the GC column (ca. 1 mL min^{-1}), a restrictor capillary tube was used between the head of the column and the TMR, which was of different dimensions according to the pressure used in the TMR. Moreover, head column pressures (BP2) were adjusted according to the carrier gas employed. Table 1 shows the settings (restrictor tubes and head column pressures) applied in every case.

To ensure a proper carrier gas split from the GC column to the detectors (MS and FID), a dedicated configuration was necessary for each carrier gas employed. A detailed scheme of the py-GC–MS/FID configurations used for helium and hydrogen can be found in the Supplementary Information, Fig. S1 and Fig. S2.

The carrier gas flow rate (He and H_2) used in the TMR was 50 mL min^{-1}. The inlet temperature of the GC was 280 °C and the split ratio in the interface was 1:50. The pyrolysis products were separated in the GC using a Restek capillary column (Rtx-1707, 60 m L × 0.25 mm I.D. × 0.25 μm d_f); the stationary phase had a mass fraction of 14% cyanopropylphenyl and a mass fraction of 86% dimethyl polysiloxane. The GC oven temperature was set to the following ramp program: 3 min hold at 40 °C followed by heating to 270 °C at the rate of 4.1 °C min^{-1} and a final temperature of 270 °C held constant for 1 min. The MS transfer line temperature was 280 °C, the ion source temperature was kept at 250 °C and the electron ionization energy was 70 eV. The FID operated at a base temperature of 250 °C and an ignition threshold of 0.5 pA. A hydrogen generator (H2PEM −100, Parker Balston, 99.9999% purity) was used to generate hydrogen for the FID. The flow of air, hydrogen and nitrogen used in the FID were 350, 35 and 30 mL min^{-1} respectively.

For processing the data, Thermo Scientific Xcalibur (version 4.2.28.14) was used for the peak area integration and the NIST Tandem Mass Spectral Library (version 2.3) was employed for the peak identification. All integrated peaks with an area of at least >0.4% were identified using the MS chromatograms, and quantified using the FID chromatograms (when possible). In the following section, the calibrations used for the quantification of the hydropyrolysis volatiles is discussed.

2.3. Calibration of the py-GC–MS/FID

The micro-pyrolysis set-up was calibrated both under helium and hydrogen; the list of calibrations can be found in the Supplementary Information in Table S2 (for He) and Table S3 (for H_2). The selection of the compounds to be calibrated was based on the compounds identified in the mass spectra obtained from micro-pyrolysis of lignocellulosic biomass with and without chloride molten salts. All the calibrations points were obtained from injections at 0.4 MPa and at 350 °C and the constructed calibration curves had a $R^2 > 0.97$. It is important to highlight that there were different approaches used for calibrating the selected compounds.

First, standard solutions of mixtures (up to 5 compounds) were prepared based on their chemical compatibility, distinct retention times and solubility with the selected solvent (either acetonitrile, water, or ethanol); the mixtures were diluted 1:1 up to 5 times. Similarly to the biomass or biomass-molten salts' sample injection, stainless-steel cups were used to introduce the mixtures of calibration compounds (2 μL from each dilution) into the micro reactor. Direct injections (i.e. non-diluted) to the micro reactor were another alternative because of the high volatility of certain calibration compounds and the otherwise inevitable overlap with the solvent peak in the chromatograms (e.g. 2-methyl furan). Calibration curves were also constructed based on the effective carbon number (ECN) theory. The ECN theory uses relative response factors from the FID, hence existing data points from the calibrations described above were used to construct new curves [22].

The quantification of non-condensables gases was not possible in this study, with the exception of CO_2 and chloromethane. Given that CO_2 can be only detected in the MS chromatograms and not in FID chromatograms, the CO_2 yields reported are semi-quantitative (i.e. GC peak area per μg of sample of CO_2). Particularly for the calibration of chloromethane (boiling point of −24.2 °C) the approach taken consisted of the injection of a syringol-salt B mixture (knowing that it would form chloromethane as a side-product through a reaction with both the methoxyl groups); from the yield of non-reacted syringol attained, the yield of chloromethane was calculated.

Table 1
Micro-reactor settings required based on pressure and carrier gas applied.

Restrictor capillary tube and TMR (BP1) pressure		Head GC column pressure (BP2)	
0.3–0.1 MPa	0.1–3.0 MPa	Helium	Hydrogen
4 m L × 0.15 mm ID	0.5 m L × 0.07 mm I.D.	0.145 MPa	0.08 MPa

2.4. Molten salts micro-pyrolysis studies

Importantly, to avoid continuing salts volatilization from the molten salts micro-pyrolysis experiments in the tandem micro-reactor [11], the temperature in the TMR was reduced from the starting reaction temperature to 200 °C approximately 1 min after the sample injection, when the biomass (hydro) pyrolysis reactions were certainly completed. The micro-pyrolysis experiments, both with and without molten salts, were performed in duplicates and standard deviations were determined per individual compound as well as per chemical group. One important limitation with molten salts micro-pyrolysis experiments occurred because both feedstock types, but especially the molten salts can be somewhat heterogeneous in the low quantities used. Nevertheless quantification in the GC–MS/FID however does provide a consistent and reproducible output throughout the experiments.

2.4.1. Carrier gas: Helium (pyrolysis)

In our previous research, molten salts pyrolysis of lignocellulosic biomass was conducted in a Py-GC–MS configuration, obtaining semi-quantitative results [11]. In this study, a Py-GC–MS/FID configuration (described in the SI, Fig. S1) was used to perform pyrolysis of pinewood and wheat straw anew with salt B to obtain quantitative yields because a benchmark is required for judging properly the subsequent hydropyrolysis (i.e. under H_2 atmosphere) experiments. These experiments were conducted at 0.4 MPa pressure, 350 °C and a biomass mass fraction in the salt B and biomass mixture of 0.09.

2.4.2. Carrier gas: Hydrogen (hydropyrolysis)

To optimize hydropyrolysis of lignocellulosic biomass in molten

Table 2
Experimental design of lignocellulosic feedstock hydropyrolysis in molten salts (salt B which is composed of $ZNCl_2$:KCl:NaCl in a mol ratio of 44.3–41.9-13.8 mol%).

experiment	pressure (MPa)	mass fraction of biomass in salt B-biomass mixture (wt%)	temperature (°C)
1 [a,b]	0.4	9	350
2 [a,b]	1.6	9	350
3 [a,b]	3.0	9	350
4 [a]	3.0	16	350
5 [a]	3.0	24	350
6 [a]	3.0	24	400
7 [a]	3.0	24	450

Conditions: [a,b] tested for pinewood and wheat straw; [a] tested for pinewood only.

chloride salts (salt B), different process conditions have been investigated (see Table 2). First, the effect of pressure (0.4 to 3.0 MPa) and mass fraction of biomass in the biomass-salt B mixture (0.09 to 0.24 wt %) were studied at 350 °C. Under atmospheric pressure conditions, 350 °C is the maximum pyrolysis temperature that can ensure no hydrolysis occurrence (HCl formation) [21], and/or salts volatilization as observed in our previous molten salts pyrolysis study. Nevertheless, Niazi et al. (2020) [23] have suggested that high-pressure hydropyrolysis can supress salt volatilization and HCl formation, which could allow operating temperatures for hydropyrolysis to increase above 350 °C. To confirm this, modelling and experimental work was conducted. HCl formation and $ZnCl_2$ volatilization from salt B were assessed at 0.1, 1.6 and 3.0 MPa by modelling in FactStge 7.2 employing FactPS and Factsalt as databases. Upon model-based confirmation (in regards to HCl formation and $ZnCl_2$ volatilization), subsequent high-pressure hydropyrolysis of biomass with salt B was investigated in the micro-reactor at higher temperatures (up to 450 °C) in combination with higher pressures as detailed in Table 2.

Finally, the effect of the individual salts constituting salt B ($ZnCl_2$, KCl and NaCl) on lignocellulosic biomass hydropyrolysis was also assessed to identify to which extent each salt constituent has a catalytic effect in biomass hydropyrolysis. For these experiments, pinewood was mixed individually with pure $ZnCl_2$, KCl and NaCl, based on a mass fraction of biomass in salt B of 0.4.

The volatiles, carbon in volatiles and oxygen yields from these experiments were calculated as follows:

$$\text{volatiles (wt.\%)} = \frac{\sum \mu g_{\text{products}}}{\mu g_{\text{biomass}}} \times 100$$

$$\text{carbon in volatiles (wt.\%)} = \frac{\sum \left[\mu g_{\text{compound}} \times \left(\frac{\text{atomic mass C} \times \text{C number}_{\text{compound}}}{\text{MW}_{\text{compound}}} \right) \right]_i}{\text{ug}_{\text{biomass}} \times \text{C fraction}_{\text{biomass}}} \times 100$$

$$\text{oxygen (wt.\%)} = \frac{\sum \left(\mu g_{\text{compound}} \times \text{O number}_{\text{compound}} \times \text{atomic mass O} \right)_i}{\sum \left(\mu g_{\text{compound}} \times \text{MW}_{\text{compound}} \right)_i} \times 100$$

The yields have been determined on dry feedstock basis.

2.4.3. Model compounds

To have a better understanding of the reaction mechanisms involved in molten salts pyrolysis, micro-pyrolysis of model compounds were conducted without salt B and with salt B, both under helium and hydrogen atmospheres (0.4 MPa, 350 °C). The model compounds were representative of the main constituents in the lignocellulosic biomass and/or of their primary pyrolysis compounds; these included: levoglucosan (Sigma Aldrich, 99%), xylan (Sigma Aldrich, from beechwood ≥90% HPLC), cellulose (Sigmacel®), furfural (Sigma Aldrich, 99%), 4-vinyl guaiacol (Sigma Aldrich, analytical standard), guaiacol (Acros organics, 99 + %), syringol (Sigma Aldrich, 99%) and creosol (Sigma Aldrich, ≥ 98%).

The preparation of the model compound samples was similar to that of lignocellulosic feedstock described in section 2.1. In this case, approximately 100 to 250 μg of each model compound was weighted into the eco-cups. For the micro-scale experiments with molten salts, approximately 1011 to 2527 μg of salt B were added and dry mixed. The latter corresponded to a model compound mass fraction of 0.09 in the mixture with salt B (wt%/wt%). For the model compounds that were liquid, a syringe was used to add and weigh them in the eco-cup.

3. Results

3.1. Pyrolysis (He) of lignocellulosic biomass in molten $ZnCl_2$:KCl:NaCl salts

Pyrolysis of pinewood (PW) and wheat straw (WS) was performed at 350 °C (py-GC–MS/FID with helium) in a tandem micro reactor with and without molten chloride salts ($ZnCl_2$:KCl:NaCl - 44.3:41.9:13.8 mol%, named salt B). All the reported volatiles' yields included in this section are on dry biomass basis. The yield of volatiles obtained from pyrolysis of pure PW and WS as well as from PW and WS with salt B were similar (Table 3).

The quantitative micropyrolysis results (Table 3) show however a different trend to that observed in our previous work on semi-quantitative micropyrolysis of PW and WS with salt B [11]. In semi-quantitative micropyrolysis of PW and WS, the volatiles' output decreased by 62% and 66% respectively with the addition of salt B. The difference in the observed trends can be explained by the different mass fraction of biomass used in the biomass-salt B mixtures. While in the previous research a mass fraction of biomass of 0.05 was used (i.e. 0.95 mass fraction of salt B), in the current study the mass fraction of biomass was increased to 0.09. Increasing the mass fraction of biomass in the sample therefore demonstrated to be beneficial to improve the volatiles' yield because the inhibition of the biomass volatilization by the "excess" molten salts was reduced. Excessive molten salts create a barrier that impedes the diffusion of pyrolysis volatiles out of the reaction medium. Moreover, the advantageous catalytic effect of salt B observed in PW and WS micropyrolysis was not affected by lowering the quantities of salt B used (down to 91 wt% at this point) as can be analyzed next in Fig. 2.

3.1.1. Carbon distribution of volatiles

The volatiles produced from pinewood and wheat straw pyrolysis with and without salt B were grouped based on their carbon number ranging from C_1 to C_{10} in Fig. 2. In this figure, the catalytic effect of salt B in PW and WS pyrolysis can be observed by the carbon fractions' selectivity. While pure PW and WS pyrolysis yielded products ranging from C_2 to C_{10} compounds, the major fraction of the products in the presence of salt B constituted C_5 and C_2 compounds. Furfural was the main product from the C_5 compounds obtained with the addition of salt B; its yield was 30.5 ± 1 wt% in PW and 30.6 ± 2 wt% in WS, while the remaining C_5 compounds consisted of 2-methyl furan and 3-methyl furan. The second major product from PW and WS pyrolysis with salt B was acetic acid which accounted for all the C_2 compounds that were possible to quantify; its yield was 18 ± 0.3 wt% in PW and 15 ± 0.8 wt% in WS. Wheat straw contains elevated levels of alkali and alkaline earth metals (shown later in 3.1.3), which are known to catalyze the decomposition of cellulose and anhydrosugars towards lighter oxygenates like acetic acid, char and non-condensable gases [24]. As such wheat straw pyrolysis yields more acetic acid (in the C2 fraction) compared to pinewood at the expense of anhydrosugars (like levoglucosan, in the C6 fraction) as can be seen from Fig. 2.

These results are similar to those reported by Sridharan et al. (2022) with respect to the product selectivity attained with chloride molten salts pyrolysis of pinewood, executed in a gram scale batch reactor heated with a fluidized sand bath [25]. Nevertheless, the yield of the main products from PW pyrolysis with chloride molten salts in their bench scale set-up at 350 °C (5 wt% ca. furfural and 7 wt% ca. acetic acid) were lower from those obtained in this study. These differences are expected because of the different heating rates and especially the hot vapor residence times attained in each reactor. Hot vapor residence times in a gram scale reactor (e.g. fluidized sand bed, ~ 1.6 s) are about

Table 3
Volatiles yields obtained from pinewood and wheat straw pyrolysis with salt B ($ZNCl_2$:KCl:NaCl composed of 44.3–41.9-13.8 mol%); conditions 350 °C, 0.4 MPa helium, mass fraction of biomass in the sample was 0.09.

	volatiles yield (wt.%) [¥]			
	pure		with salt B	
pinewood (PW)	54.8	± 0.8	54.8	± 2.1
wheat straw (WS)	53.5	± 2.4	52.7	± 0.6

[¥] mass of volatiles per mass of biomass on dry basis.

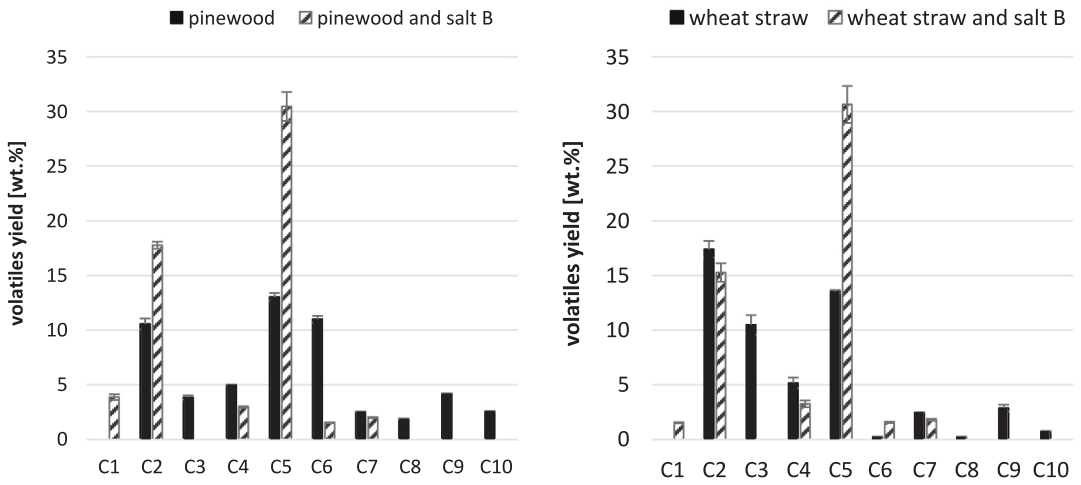

Fig. 2. C_1-C_{10} compound yield obtained from pinewood and wheat straw pyrolysis with and without salt B ($ZnCl_2$:KCl:NaCl composed of 44.3–41.9-13.8 mol%); conditions: 350 °C, 0.4 MPa helium, mass fraction of biomass in the sample was 0.09.

2 orders of magnitude longer compared to a milligram scale reactor (e.g. screen-heater in [26], ~ 0.02 s), which results in significant cracking of the vapors. Therefore, because of the lower hot vapor residence time attained in the micro reactor, secondary reactions of products outside the reacting particle were limited, and the mass yield of furfural and acetic acid obtained (i.e. condensable vapors/volatiles) was higher.

3.1.2. Pyrolysis of model compounds

To comprehend more the catalytic effect of chloride molten salts, py-GC–MS/FID tests of model compounds related to the holocellulose and lignin fraction from lignocellulosic biomass were performed at 350 °C (Table 4 and Table 5). The list of model compounds included levoglucosan (LG), cellulose (CEL), xylan (XYL), vinyl guaiacol (V-GUA),

Table 4
Py-GC–MS/FID of holocellulose-related model compounds with and without molten salts under helium atmosphere at 350 °C and 0.4 MPa helium. **LG**: levoglucosan, **XYL**: xylan, **CEL**: cellulose, **SB**: Salt B (composed of $ZnCl_2$:KCl:NaCl in 44.3–41.9-13.8 mol%). The yields in wt% represent the mass of volatiles per mass of model compound on dry-basis. **Highlighted (i.e. in bold font) yields** in the table are of relevance and discussed in text.

Group	Compound	LG (wt.%)	LG – SB (wt.%)	XYL (wt.%)	XYL – SB (wt.%)	CEL (wt.%)	CEL – SB (wt.%)
	methanol			++	++		
Alcohols	1,3-butanediol			++			
	2-propenol			2.0			
	pentanal			++			
Aldehydes	methyl glyoxal	++	++				
	acetaldehyde			0.9	0.9		1.7
	levoglucosan	**70.1**				**45.2**	
	levoglucosenone					1.3	
Anhydro-sugars	1,4:3,6-dianhydro-α-D-glucopyranose					++	
	2,3-anhydro-d-mannosan	++					
	3,4-anhydro-d-galactosan	++					
	2,3-anhydro-d-galactosan	++					
	acetic acid		**11.1**	**2.0**	**2.4**		**7.4**
Carboxylic acids	propanoic acid			3.6			
	2-propenoic acid			3.1			
	pyruvic acid			++			
Esters	2(5H)-furanone					0.8	
Ethers	3-methyl-2,5-furandione		++	++	++		
	ethyl propenyl ether			++			
	furfural		**63.1**	**13.3**	**22.8**	**12.6**	**29.6**
	5-hydroxymethylfurfural					0.4	
	5-methyl furfural		2.8				1.0
Furans	2-methylfuran		++				++
	3-methylfuran		++				
	furan		++		++		++
	acetylfuran		**1.2**				**0.5**
Halogens	chloromethane				0.5		
	acetone		11.5	2.8	4.8		4.0
	hydroxyacetone			4.1			
	3-methyl-1,2-cyclopentanedione			++		++	
Ketones	2,3-butanedione		4.7	1.1			1.6
	1-hydroxy-2-butanone			++			
	3-pentanone			++			
	2,3-pentanedione			++			
Pyrans	5-hydroxymaltol					++	
	total volatiles (wt.%)	**70.1**	**94.3**	**33.0**	**31.4**	**60.4**	**45.8**

++ was detected with a peak area > 1%, but could not be quantified.

Table 5
Py-GC–MS/FID (yield in wt%) of lignin-related model compounds with and without molten salts under helium atmosphere at 350 °C and 0.4 MPa helium. **V-GUA**: 4-vinyl guaiacol, **GUA**: guaiacol, **SYR**: syringol, **SB**: Salt B (composed of $ZnCl_2$:KCl:NaCl in 44.3–41.9-13.8 mol%). **Highlighted yields** in the table are of relevance and discussed in text.

Group	Compound	V-GUA (wt%)	V-GUA + SB (wt%)	GUA (wt%)	GUA + SB (wt%)	SYR (wt%)	SYR + SB (wt%)
Alcohols	methanol		++		++		++
	3-methylcatechol		1.1				
Alkyl phenols	4-methylcatechol		1.0				
	4-ethylcatechol		1.1				
Halogens	chloromethane		**3.8**		**0.2**		**2.8**
	creosol	1.9	**1.3**				
	guaiacol	3.2	**15.0**	**74.1**	**63.8**		
	4-vinyl guaiacol	**47.3**					
	p-ethylguaiacol	1.7	**3.3**				
	isoeugenol	6.0					
Methoxy phenols	vanillin	1.3	1.3				
	cis-isoeugenol	0.4					
	2-methoxy-4-methyl-6-[(1E)-1-propenyl]phenol		0.7				
	isocreosol		1.1				
	4-methoxy-3-methylphenol		1.1				
	syringol					**84.5**	**82.5**
	phenol				0.3		
Mono-aromatics	o-dimethoxybenzene		1.1				
	2,5-dimethoxyethylbenzene		0.3				
Naphtols	3-methoxy-2-naphthol		++				
Phenols	catechol		2.5				
Quinones	hydrothymoquinone		2.4				
	total volatiles (wt.%)	**61.8**	**37.2**	**74.1**	**64.3**	**84.5**	**85.3**

++ was detected with a peak area > 1%, but could not be quantified.

guaiacol (GUA) and syringol (SYR).

3.1.2.1. Holocellulose derived. This sub-section deals with the catalytic effect of chloride molten salt (salt B) during pyrolysis of LG, CEL and XYL. In essence, it is shown that salt B catalyzes the reaction pathways of LG, CEL and XYL and promotes furfural above all in the condensable fraction. Predominantly, furfural was found to be formed as a secondary decomposition product from LG.

Table 4 shows that at 350 °C, LG hardly decomposes and yields mostly volatilized LG (70 wt%) similar to the study of Patwardhan et al. (2011) [27]. Conversely, with the addition of salt B, the pyrolysis products from LG consisted of furans (mainly furfural), carboxylic acids (acetic acid) and ketones (acetone, 2,3-butanedione). Most likely in the presence of salt B, the decomposition of LG occurred first by the ring-opening of the glycosidic 1,6-acetal bond and the rehydration to form the glucopyranose monomer followed by secondary reactions. The secondary reactions could include 1) cleavage of the pyran ring to the hexose chain structure, 2) dehydration of the OH- groups and 3) acetal reaction on C-2 and C-5, which produces 5-HMF as an intermediate; 5-HMF would then decompose into furfural [28]. The high acetic acid production (11 wt%) from LG pyrolysis in salt B can derive from promoted LG secondary reactions in which hydroxyacetaldehyde is 1) produced, 2) dehydrates to a ketene structure and 3) rehydrates to form acetic acid [28]. The formation of acetyl furan from pyrolysis of LG (and CEL) with salt B can be formed from 6-deoxyaldohexose dehydration in the presence of a Lewis acid such as Cr^{3+} [29]. In this case, the 6-deoxyaldohexose would correspond to 6-deoxy-D-glucopyranose (glucopyranose with one —OH replaced by —H) and the Lewis acid is $ZnCl_2$ within salt B.

In accordance with previous publications, the main CEL pyrolysis products consisted of anhydrosugars -predominantly levoglucosan (45 wt% in this study)- and furfural. Formic acid or glycolaldehyde however were not detected at a reactor temperature of 350 °C which was used in this study [26,27]. Levoglucosan is formed from CEL pyrolysis through a hydroxyl-catalyzed transglycosylation mechanism, which is suggested as the primary route for cellulose activation at lower pyrolysis temperatures (< 467 °C) [30]. On the other hand, as expected CEL pyrolysis with salt B did not produce any anhydrosugars and instead, led mainly to the formation of furans (predominantly furfural but also 5-methyl furfural, methyl furan, furan and acetyl furan). The selective production of furfural showed that molten chloride salts (salt B) promoted ring opening/fragmentation reactions and dehydration reactions from the glucopyranose structure. The fact that not only furfural was selectively produced from CEL pyrolysis with salt B but also its yield increased more than twice (~ 13 wt% - > ~ 30 wt%), suggests that LG was produced as an intermediate product and this further converted into furfural.

Salt B in CEL pyrolysis also promoted the production of light oxygenated compounds, such as acetic acid and acetone. Without molten salts, acetic acid is formed from degraded fragments derived from cellulose depolymerization which undergo ring scission, thereby producing acetic acid by deacetylation of the fragments [31]. Interestingly, Table 4 shows that in presence of salt B, the acetic acid yield was higher in CEL (~ 7 wt%) compared to XYL (~ 2 wt%); this further supports that LG was an intermediate product in CEL pyrolysis with salt B because the generated LG likely decomposed into acetic acid by secondary cracking reactions such as ring scission and deacetylation, consequently increasing the acetic acid yield [31].

Usually, the product portfolio from purified hemicellulose (ash content <0.1 wt%) pyrolysis consists of 1) low molecular weight compounds (CO, CO_2, formic acid, acetaldehyde, acetic acid and acetol), 2) furan/pyran ring derivatives and 3) anhydrosugars (dianhydroxylopyranose, anhydroxylopyranose) at 500 °C [24]. Xylan obtained from beechwood was used as a proxy for hemicellulose. Similar to Patwardhan et al. (2011), the ash in the beechwood derived XYL (8.3 wt% ash content) significantly affected the pyrolysis products yields, especially because no anhydrosugars derived from xylose were detected. The high ash content in XYL (with substantial alkali and alkaline earth metals -AAEMs) promoted ring-scission reactions which led to the formation of light oxygenates and non-condensable gases (not measured), as well as dehydration reactions contributing to the formation of furfural and char, and at the expense of the production of anhydrosugars [24].

Compared to CEL or LG, a higher yield of char and non-condensables from XYL pyrolysis can explain the lower overall yield attained from the latter. Although char yields were not measured, CO_2 yields (normalized GC area response) from XYL were substantially higher than in CEL or LG (as shown in Fig. S3 in the appendix). Patwardhan et al. (2011) also

showed that the content of the alkaline earth metals (2222 ppm (mg kg^{-1}) K and 17,980 ppm (mg kg^{-1}) Na) in XYL caused a slight increase in the acetaldehyde yield (compared to purified hemicellulose) whereas all AAEMs contributed to formic acid and acetol decrease. In this study, the acetaldehyde and acetol (or hydroxyacetone) yields are within the range of those previously reported which supports the catalytic activity inflicted by the AAEMs present in XYL. However, Table 4 shows that formic acid was not a main product from XYL pyrolysis at 350 °C as previously reported with yields ranging between 7 and 11 wt% [24]. Although formic acid was not quantified in the FID, traces of formic acid (*m/z* 45, 46) were detected in the MS. The addition of salt B in XYL pyrolysis showed to promote even more depolymerization, rearrangement and dehydration reactions leading to an increase in furfural yield (13 wt% - > 23 wt%) similar to CEL pyrolysis with salt B.

3.1.2.2. Lignin derived. Vinyl guaiacol (V-GUA), guaiacol (GUA) and syringol (SYR) were chosen as the model compounds to observe the interaction between the lignin fraction (or intermediates thereof) of lignocellulosic biomass (PW and WS) and salt B (Table 5). From the overall volatile yields, it is observed that salt B was reactive towards the model compounds in the following order V-GUA > > GUA > SYR. Especially in the case of V-GUA, it is evident that the molten salts promoted the formation of char and non-condensable gases over the volatiles. The three model compounds reacted with salt B and formed chloromethane (CH_3Cl) as a pyrolysis by-product at 350 °C; the CH_3Cl yield was prominent in the following order V-GUA > SYR > > GUA. The formation of CH_3Cl more specifically derived from the reaction of methanol and HCl as indicated in eq. 1. This was demonstrated in our previous study [11]. In essence, the eutectic chloride mixture salt B catalyzed demethoxylation reactions of methoxyphenols like 4-vinylguaicol and guaiacol, generating methyl groups that in the presence of water formed methanol. Hydrochloric acid on the other hand, was formed from the salts' hydrolysis in the presence of water as shown in eq. 2, where M stands for metal (like Zn) and X for halides. Although salt B was deep dried at 300 °C prior its use to prevent water being present in the molten salt and thus to reduce subsequent salt hydrolysis, water formed from biomass dehydration reactions still led the salts to hydrolyze and form HCl.

$$CH_3OH + HCl \rightarrow CH_3Cl + H_2O \quad (1)$$

$$MX_2 + H_2O \rightarrow MO + 2HX \quad (2)$$

The interaction between salt B and the lignin-derived model compounds supports the reaction mechanisms proposed for Lignoboost Kraft lignin and salt B in our previous publication [11]. Essentially, salt B promoted demethoxylation of GUA to a certain extent, which formed phenol and methanol. Moreover, salt B completely decomposed V-GUA through cracking reactions which mainly produced guaiacol (15 wt%). Since creosol is formed in both V-GUA pyrolysis with and without salt B in comparable yields (1.3 to 1.9 wt%), it is fair to suggest that salt B does not contribute in this particular reaction mechanism of V-GUA. Salt B also promoted demethoxylation of SYR to a limited extent (SYR yield decreased by 2 wt%), given the methanol production (starting point for CH_3Cl formation, also formed). However, since guaiacol was not detected from SYR pyrolysis in salt B, it is likely that the reactive SYR fraction was fully converted to char.

3.1.3. Effect of molten salts on the chemical portfolio

The vapor phase product distribution -based on chemical group association- is compared between PW and WS with and without salt B in Fig. 3. The list of compounds from each chemical group is detailed in Table S4 from the SI. What can be clearly seen in this figure is the dramatic increase in furans in PW and WS pyrolysis when the chloride molten salts have been added, which is also clear from the increment in the C_5 fraction (Fig. 2). In both cases with the presence of salt B, the furans yields were 18.4 wt% higher compared to the pure feedstock pyrolysis, which led to a total furans yield between 32 and 32.6 wt%. The enhanced furans production (mainly furfural) stemmed from the catalytic activity that salt B has on the primary and secondary reactions from cellulose and hemicellulose fractions of the feedstock, as shown in Table 4 from the model compounds. The effect that molten salts have in both primary and secondary reactions cannot be disentangled. However, it is certain that molten salts catalyzed secondary reactions of intermediates (like 5-HMF produced in PW) into furfural.

The production of carboxylic acids (acetic acid) had a different trend in PW and WS with the addition of salt B. While carboxylic acids from PW pyrolysis increased with salt B, the trend was opposite for WS. During pyrolysis (without salts), acetic acid is mainly produced from deacetylation of hemicellulose, but is also expected from the thermal cracking of cellulose [31]. A higher hollocellulose fraction (especially hemicellulose) in WS could explain the higher production of carboxylic acids from WS pyrolysis compared to that from PW, but this is not the case. Both the hemicellulose fraction in PW (27 wt%) is fairly comparable to that in WS (25 wt%); and the cellulose fraction in PW (46 wt%) is also comparable to that in WS (45%) [32,33]. The observed larger yield in carboxylic acids from pure WS pyrolysis however can be attributed to higher quantities of ash forming elements in WS compared to PW. In parallel, this also explains the lack of anhydrosugars

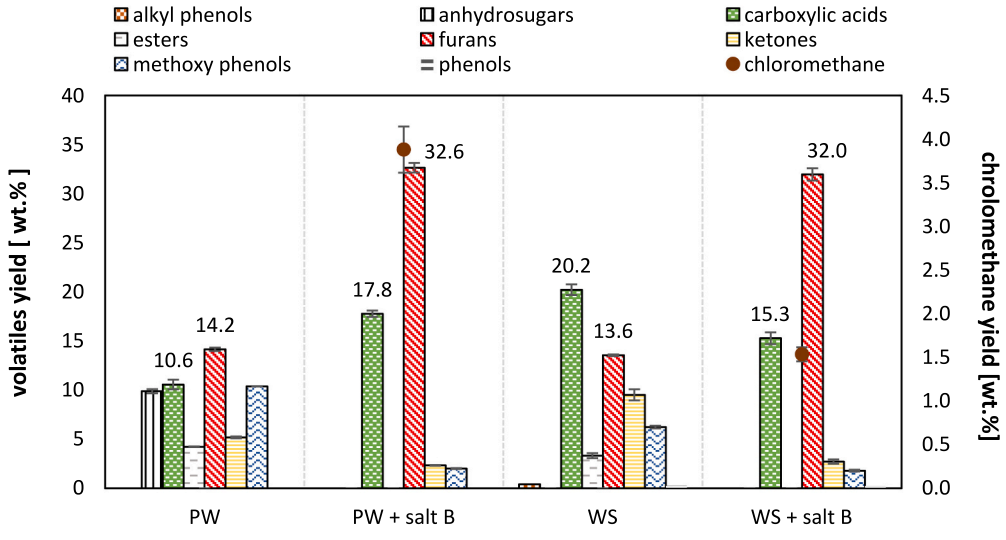

Fig. 3. Distribution of chemical groups in pinewood and wheat straw pyrolysis with and without salt B ($ZNCl_2$:KCl:NaCl composed of 44.3–41.9-13.8 mol%); conditions: 350 °C, 0.4 MPa helium, mass fraction of biomass in the sample was 0.09. Actual values of furans and carboxylic acid yields have been indicated as the major compound groups. Chloromethane yields are depicted as circles and can be read in the secondary y-axis. (For the list of individual compounds included within each group, the reader is referred to Table S4 from SI).

production from WS, opposite to what was observed from PW. The composition of the ash forming elements in PW and WS is shown in Table 6.

Patwardhan et al. (2010) have proven that very small amounts of AAEMs (particulary K^+, Na^+, Mg^{2+}, Ca^{2+}) present in the ash alter pyrolysis products, leading to a decline of anhydrosugars (mainly levoglucosan) and formation of low molecular weight species (like formic acid, glycolaldehyde and acetol). The suggested order of the AAEMs effect on levoglucosan yield follows $K^+ > Na^+ > Mg^{2+} > Ca^{2+}$ [35]. These observations are confirmed by comparing the pyrolysis of pure WS and PW in this study and their AAEMs quantities (shown in Table 6). Specifically, the high content of potassium in WS most likely catalyzed secondary reactions of anhydrosugars (mainly levoglucosan) from WS pyrolysis, leading to higher acetic acid yields in WS (17.4 wt%) compared to PW (10.6 wt%) as shown in Table S4. In parallel, low molecular species such as acetol (or hydroxyacetone) increased in pure WS (7.7 wt%) compared to pure PW (3.8 wt%) (shown in Table S4 in SI), which also reflected the effect of the AAEMs in the secondary decomposition of levoglucosan [28]. Consequently, without the interaction of the ash forming elements in the original primary pyrolysis compounds derived from PW (levoglucosan production mainly), there was more pronounced acetic acid production from PW with salt B (18 wt% ca.) compared to WS with salt B (15 wt%), as a result from salt-catalyzed secondary reactions of levoglucosan from PW.

The primary methoxyphenols from pyrolysis of PW (10.4 wt%) and WS (6.2 wt%) at 350 °C were 4-vinyl guaiacol > guaiacol > cis/trans isoeugenol. The higher yield of methoxyphenols from PW pyrolysis was mainly because of a higher content of 4-vinyl guaiacol produced (4 wt %), compared to WS (3 wt%). From the results observed with the lignin-related model compounds (Table 5), the methoxyphenols' formation was expected to decline with the addition of salt B. Salt B promoted cracking and demethoxylation reactions of 4-vinyl guaiacol, guaiacol and cis/trans isoeugenol formed during PW and WS pyrolysis, which consequently formed guaiacol (solely) as well as methanol and most likely ethylene/propylene (not detectable in the current configured set-up). The more pronounced decrease in the methoxyphenols' total yield from PW compared to WS in the presence of salt B can explain the higher CH_3Cl formation from PW compared to WS, stemming from the higher methanol production from demethoxylation reactions of the phenolics in PW. With salt B, the quantified yield of methoxyphenols (consisting only of guaiacol) from both PW and WS was ca. 2 wt%.

Regarding the ketones, these are typically formed from intermediates such as anhydrosugars. Especially in WS, which has more AAEMs, the anhydrosugars are broken down to more ketones (like acetone, hydroxyacetone). As the salts catalyze a different reaction starting from the anhydrosugars or precursors thereof, there are no more or fewer anhydrosugars left to decompose into ketones. Hence, it makes sense that the ketones are quite suppressed in the presence of the salts, but are elevated without the salts (especially in WS).

Overall, this sub-section explored the influence of salt B on the product distribution from pinewood and wheat straw pyrolysis. Furan-ring compounds followed by carboxylic acids were the dominant chemical species from pyrolysis of these biomasses in the presence of salt B.

Table 6
Elemental analysis for pinewood and wheat straw samples. Main values have been highlighted [34].

Element	Pinewood (wt%)	Wheat straw (wt%)
Al	0.004	0.023
Br	<0.10	<0.10
Ca	**0.11**	**0.27**
Cl	0.14	0.51
Fe	0.012	0.029
K	**0.032**	**0.91**
Mg	**0.023**	**0.052**
Mn	0.013	0.003
Na	**0.005**	**0.008**
P	0.003	0.024
Si	0.026	0.95
Ti	0.001	0.001

3.2. Optimization of hydropyrolysis of lignocellulosic biomass in molten $ZnCl_2$:KCl:NaCl salts

Hydropyrolysis of pinewood (PW) and wheat straw (WS) with molten chloride salts (salt B) was performed in a tandem micro reactor (py-GC–MS/FID with hydrogen); the effect of 3 process variables was investigated in this section: pressure, biomass mass fraction in the biomass-molten salts mixture and temperature. The effect of pressure (0.4–3.0 MPa) in molten salts hydropyrolysis was investigated for both PW and WS. Nonetheless, the effect of the mass fraction of biomass in the biomass-salt B mixture (0.09–0.24) and temperature (350–450 °C) in molten salts hydropyrolysis was investigated solely for PW, to focalize the research.

Firstly, pressure was investigated mainly to find an optimal condition for hydrogenation ($+H_2$) and hydrodeoxygenation ($+H_2$, $-H_2O$) of furan-ring compounds, which are selectively produced due to salt B's catalytic effect during the biomass conversion. Secondly, as discussed in section 3.1, the lower the mass fraction of biomass used in pyrolysis of lignocellulosic feedstock with molten salts (i.e. more molten chloride salts), the more primary volatiles are hindered to be released from the mixture. Therefore, a reasonable approach was to investigate the increase of the mass fraction of biomass in the biomass-molten salts mixture. Finally, in accordance to modelling data on the chloride salts stability, the increment in molten salts hydropyrolysis temperature (> 350 °C) was tested when higher pressures were also applied. The effect of these 3 process variables on lignocellulosic biomass hydropyrolysis in molten chloride salts was assessed with respect to 1) the overall volatiles yields and 2) the hydrogenation/hydrodeoxygenation of the furanic compounds.

3.2.1. Effect of process conditions on the overall volatiles' yields

Fig. 4 and Fig. 5 show PW and WS hydropyrolysis in the presence of molten chloride salts respectively, under different process conditions. The effect of the process conditions was assessed on the volatiles yield, carbon-in-volatiles yield and oxygen-in-volatiles content attained; the char and non-condensable gases yields however could not be determined. Although, semi-quantitative CO_2 yields under the different process conditions are included. Fig. 4 and Fig. 5 show the effect of *pressure* (experiment number 1 to 3) for PW and WS respectively, while Fig. 4 additionally shows the effect of *mass fraction of biomass in the biomass-salt B mixture* and *temperature* for PW (experiment number 4 to 7).

Before examining the effect of the different process conditions on hydropyrolysis with molten salts, it is important to highlight the influence of the reaction atmosphere (H_2 and He) on the volatiles yield from lignocellulosic biomass. The total yield of pyrolysis volatiles attained at 350 °C (Table 3) was higher than the total yield of hydropyrolysis volatiles (Fig. 4 and Fig. 5). The differences in volatiles' yield when comparing H_2 and He atmospheres, can be observed from both pure biomass or from biomass with salt B (only at conditions of 350 °C and 0.4 MPa). For example, the total yield of volatiles from PW pyrolysis and PW hydropyrolysis (without molten salts) were ca. 55 wt% and 36 wt% respectively. Sugar intermediates in pyrolysis, which can be quite reactive, can potentially be more unstable in the hydrogen atmosphere and thus lower the recorded volatile yield, even at these fairly low temperatures. This will be evidenced further in section 3.1.2.1, where the volatile yields of the hollocellulose model compounds is assessed. Most likely then and in the presence of hydrogen, the more reactive and smaller oxygenates are converted into smaller aliphatics (like C_2/C_3) or non-condensables (CH_4), however, the latter compounds fall outside the detection of the GC–MS (with respect to the *m/z* scanning range).

These observations regarding the influence of reaction atmosphere are comparable to those of Wang et al. (2022), where it was found that

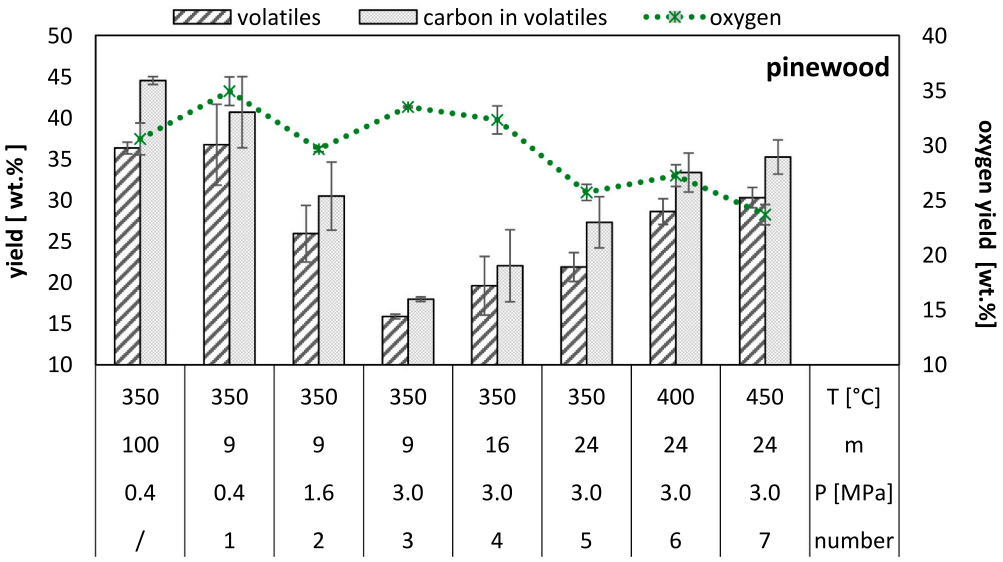

Fig. 4. Volatiles yield, carbon-in-volatiles yield and oxygen-in-volatiles mass fraction from pinewood hydropyrolysis in salt B under different process conditions (**T**: temperature, **m:** biomass mass fraction in biomass-salt B mixture, **P**: pressure); salt B is composed of $ZnCl_2$:KCl:NaCl in the ratio of 44.3–41.9-13.8 mol%.

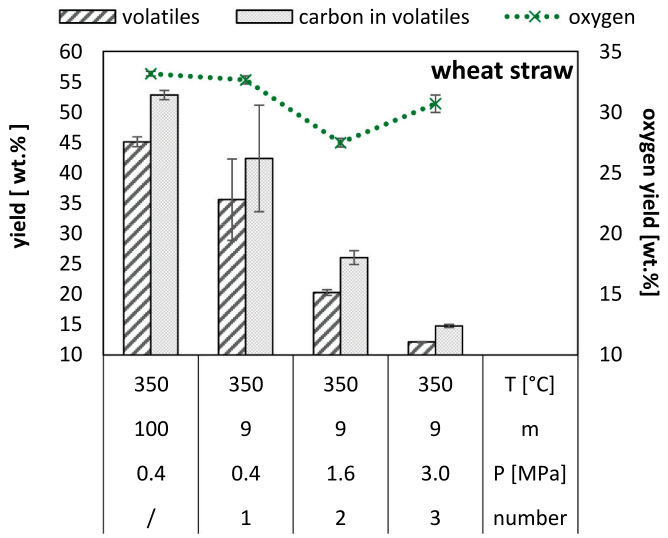

Fig. 5. Volatiles yield, carbon-in-volatiles yield and oxygen-in-volatiles mass fraction from wheat straw hydropyrolysis in salt B under different process conditions (**T**: temperature, **m**: biomass mass fraction in biomass-salt B mixture, **P**: pressure); salt B is composed of $ZnCl_2$:KCl:NaCl in the ratio of 44.3–41.9-13.8 mol%.

the C-yield was higher from cellulose pyrolysis than cellulose hydropyrolysis; the latter though was only observed at the lowest pressure tested (1.0 MPa). Under higher pressures (> 1.5 up to 3.0 MPa), they found an opposite trend, in which higher C-yields were attained under H_2 compared to He atmospheres. Similarly to their work, this study also found that H_2 changed the product distribution from lignocellulosic biomass (without molten salts), mainly because H_2 enhanced the formation of ketones (shown further in section 3.2.3) [17].

Now, clearly an increase in pressure caused a sharp decrease of the volatiles yield from PW and WS hydropyrolysis in salt B, where the volatiles' yield decreased from ca. 35 wt% at 0.4 MPa down to a range of 12 wt% (WS) to 16 wt% (PW) at 3.0 MPa (shown in Fig. 4 and Fig. 5). Therefore, high pressure-molten salts hydropyrolysis favored the formation of either non-condensable gases or char. It is possible that the formation of methane was promoted at higher pressures ($CO_2 + 4H_2 \rightarrow CH_4 + 2H_2O$) as observed from cellulose hydropyrolysis experiments conducted at 1.0 MPa (< 3%) vs. 3.0 MPa (11.8%) [17]. Although the non-condensable gases yield is unknown in this study, semi-quantitative CO_2 yield is known from the MS and is shown in Fig. S4 in the SI. This figure shows that with increasing pressure from 0.4 MPa to 3.0 MPa (experiment number 1 to 3), the CO_2 yield decreased by ca. 40% for PW and by ca. 26% for WS. This could suggest that in fact CO_2 reacted with H_2 to some extent to produce methane. He et al. (2023) has shown through kinetic studies of biomass pyrolysis with molten salts that CO and H_2 is mainly formed from lignin, CO_2 mainly from cellulose and CH_4 mainly from hemicellulose and cellulose [36]. Nevertheless, given the fact that the volatiles yield decreased at higher hydropyrolysis pressure, which is opposite to the observations of Wang et al. (2022) for cellulose hydropyrolysis, it is possible that the formation of char was more favored than that of non-condensable gases because of the diffusion barrier imposed by the molten salts during the release of volatiles combined with high-pressure conditions [17]. This was confirmed in the experiments number 3 to 5 in Fig. 4, which showed that an increase of the biomass mass fraction in the biomass-salt B mixture (i.e. less molten salts used and thus lower limitations imposed on the diffusion of volatiles out of the molten salt medium) from 9 wt% to 24 wt% resulted in a 5 wt% increase of the volatiles yield.

The study of process temperatures >350 °C for chloride molten salts pyrolysis (or hydropyrolysis in this case) was limited in our previous study because of the existing risk of salt's hydrolysis (leading to HCl production) and volatilization of $ZnCl_2$ [11,21]. These two phenomena are of relevance at analytical scale but also at larger scale. HCl formation could lead to corrosion of reactor metal vessels whereas $ZnCl_2$ volatilization could result in contamination of the condensed bio-liquids produced at larger scale reactors. Modelled hydrolysis (HCl in gas form) and volatilization ($ZnCl_2$ in gas form) from salt B however, showed that hydropyrolysis temperatures >350 °C could be used more reliably under pressures >1.6 MPa (Fig. 6). At low H_2 pressure (0.1 MPa), $ZnCl_2$ in salt B starts to volatilize after ~375 °C with rapid increase when the temperature goes to up 500 °C (Fig. 6- a). Conversely, at higher H_2 pressures of 1.6 MPa (Fig. 6 – b) and 3.0 MPa (Fig. 6– c), $ZnCl_2$ in salt B is predicted not to volatilize in the temperature range assessed (i.e up to 500 °C). Moreover, it was also evident that HCl formation from salt B was by far, much less pronounced at any temperature under H_2 pressure of 1.6 MPa or 3.0 MPa compared to 0.1 MPa. Chloride molten salts-hydropyrolysis of lignocellulosic biomass under high H_2 pressure of 3.0 MPa was thereby chosen to study the effect of elevated temperature (up to 450 °C) while simultaneously preventing volatilization and hydrolysis derived

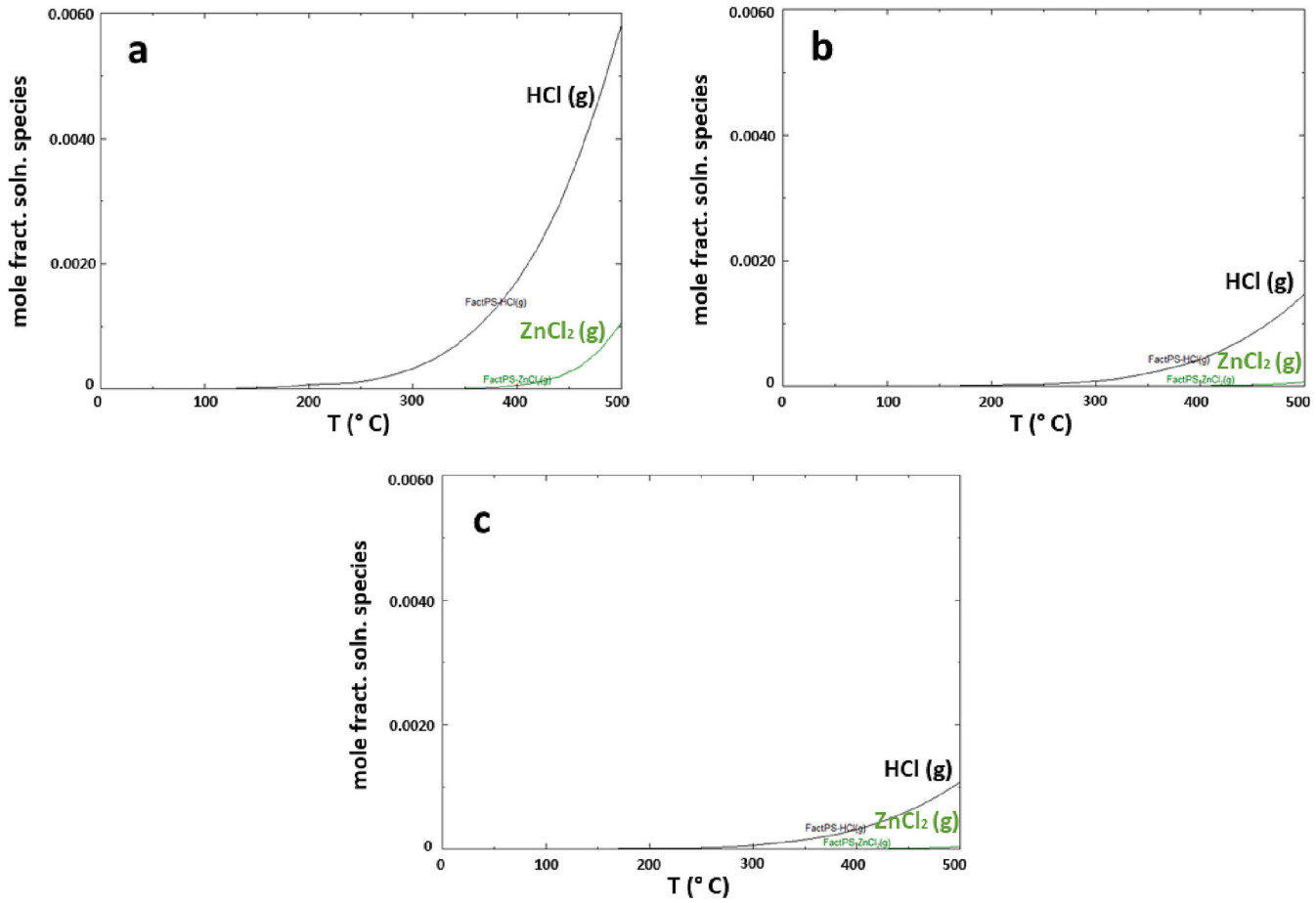

Fig. 6. Modelled hydrolysis (black curve) and volatilization (green curve) of $ZnCl_2$:KCl:NaCl molten salts (salt B) at different pressures in function of temperature. (a): 0.1 MPa, (b): 1.6 MPa and (c) 3.0 MPa. (For interpretation of the references to colour in this figure legend, the reader is referred to the web version of this article.)

phenomena (experiment number 5 to 7 in Fig. 4).

The high-pressure hydropyrolysis volatiles from PW in salt B increased from ca. 22 wt% to 30 wt% with a temperature increase from 350 °C to 450 °C. Importantly, no HCl excess (that would be detected in the chromatograms) or signs of $ZnCl_2$ volatilization were observed under the high-pressure and high-temperature conditions tested, which validated the modelled hydrolysis and volatilization behaviour of salt B (shown in Fig. 6). In spite of that, a major contributor to the mentioned increase in the volatiles yields was chloromethane, which suggests that at 450 °C the HCl formation resulting from salts' hydrolysis was more pronounced than at 350 °C.

Overall it was observed that the mass fraction of oxygen in the volatiles varied from 35 wt% down to 24 wt% (Fig. 4 and Fig. 5), where both an increase in the mass fraction of biomass in the biomass-salt B mixture and also an increase in temperature, seems to be favorable for decreasing the oxygen content in the volatiles. With the biomass mass fraction increase and especially upon temperature increase, more phenol-type volatiles were obtained (like alkyl-phenols shown in 3.2.3), because less salts were used and hence their imposed barrier to the volatiles release (which repolymerise phenol intermediates to char) was suppresed to certain extent. This can therefore explain why the overall oxygen concentration in the volatiles decreases because of the lower O content in the phenolic molecules.

3.2.2. *Hydropyrolysis of model compounds*

Similar to the assessment of chloride molten salts' catalytic effect on the pyrolysis of model compounds under helium, py-GC–MS/FID tests of model compounds under hydrogen atmosphere were also performed at 350 °C (Table 7 and Table 8). The list of model compounds included levoglucosan (LG), xylan (XYL), cellulose (CEL), furfural (FF), 4-vinyl guaiacol (V-GUA), guaiacol (GUA), syringol (SYR) and creosol (CRE).

3.2.2.1. Holocellulose derived model compounds. Different from the work of Wang et al. (2022) where levoglucosan (LG) was not observed as a hydropyrolysis product of a pure LG injection, this study did quantify LG as a hydropyrolysis product [17]. This difference most likely occurred because of the thermal instability of LG at the temperature used in their work (500 °C) compared to that of this study (350 °C).

The total quantified volatiles from pure LG hydropyrolysis at 350 °C was approximately 10 wt% lower than the yield obtained using a helium atmosphere (section 3.1.2). Although the main detected product from pure LG injection under both He and H_2 was LG itself (70 wt% and 53 wt % respectively), the by-products differed. Under H_2 atmosphere, one of the divergent by-products from LG was cyclopentenone which could have been formed from hydrodeoxygenation of furfural [17]. Another differing by-product was hydroxyacetone which can be formed as a secondary decomposition compound from LG. Importantly, it is believed that hydroxyacetone is mainly produced from direct conversion of cellulose molecules and less from secondary reactions derived from LG [28]. Nevertheless, under H_2 atmosphere, the formation of hydroxyacetone occurred from secondary decomposition of levoglucosan (4.8 wt%) or xylan (8.7 wt%) and not from direct conversion from CEL given that hydroxyacetone was not produced from this model compound (Table 7).

The catalytic effect from the chloride molten salts (salt B) observed on LG pyrolysis was also observed in LG hydropyrolysis, this being a high selectivity for furfural and acetic acid production. However, LG hydropyrolysis in salt B produced a total volatiles' yield (ca. 27 wt%)

Table 7
Py-GC–MS/FID (yield in wt%) of sugars-related model compounds with and without molten salts under hydrogen atmosphere at 350 °C and 0.4 MPa. **LG**: levoglucosan, **XYL**: xylan, **CEL**: cellulose, **FF**: furfural, **SB**: Salt B. **Highlighted yields** in the table are of relevance and discussed in text.

Groups	Compound	LG (wt%)	LG + SB (wt%)	XYL (wt%)	XYL + SB (wt%)	CEL (wt%)	CEL + SB (wt%)	FF (wt%)	FF + SB (wt%)
Alcohols	methanol			1.5	1.3				
Aldehydes	pentanal			0.1					
Alkanes	isobutane		0.3	0.3					
Alkenes	(E)-2-butene						0.5		
Anhydro-sugars	levoglucosan	**53.0**				**27.1**			
	levoglucosenone					++			
	1,4:3,6-dianhydro-α-D-glucopyranose					++			
Carboxylic acids	acetic acid		**3.0**	**2.6**	**2.9**		**3.2**		
	propanoic acid			7.3					
Esters	2(5H)-furanone	0.9				1.4			
	2-hydroxy-gamma-butyrolactone			++					
Ethers	ethyl propenyl ether			0.1					
Furans	2-methylfuran		**0.6**		**1.6**		**1.4**	**44.2**	**15.9**
	furfural		**15.7**	**3.9**	**29.0**	**3.1**	**19.6**	**54.0**	**90.9**
	2,5-dimethylfuran					0.6			
	acetylfuran		0.4				0.4		
	furan		0.6		1.2		0.8		
	5-methylfurfural		0.7			1.0	0.6		
	furfuryl alcohol				1.5	1.0			
	HMF					0.7			
	furaneol	++				++			
Halogens	chloromethane				**0.4**				
Ketones	acetone				0.6				
	2-butanone			0.1					
	cyclopentanone				0.6	0.8			
	hydroxyacetone	**4.8**	**5.1**	**8.7**	**6.3**		**4.3**		
	α-methylcyclopentanone					0.3			
	2-hydroxycyclopent-2-en-1-one					1.2			
	2-hydroxy-3-methyl-2-cyclopenten-1-one	0.3		0.2		0.5			
	2-cyclopen-1-one	1.2				1.2			
	1-hydroxy-2-butanone			2.2					
	1,2-cyclopentanedione			1.4					
	3-pentanone			0.1					
	2,3-pentanedione			++					
Phenols	phenol					0.3			
	1,4-benzenediol					0.6			
Sugars	D-allose					++			
	total volatiles quantified (wt.%)	60.2	26.5	28.5	45.3	39.8	30.8	98.3	106.8

++ was detected with a peak area > 1%, but could not be quantified.

Table 8
Py-GC–MS/FID (yield in wt%) of lignin-derived model compounds with and without molten salts under hydrogen atmosphere at 350 °C and 0.4 MPa. **V-GUA**: 4-vinyl guaiacol, **GUA**: guaiacol, **SYR**: syringol, **CRE**: creosol, **SB**: Salt B. . **Highlighted yields** in the table are of relevance and discussed in text.

Groups	Compound	V-GUA (wt%)	V-GUA + SB (wt%)	GUA (wt%)	GUA + SB (wt%)	SYR (wt%)	SYR + SB (wt%)	CRE (wt%)	CRE + SB (wt%)
Alcohols	methanol		2.1	+	0.7		1.8		0.5
Alkyl phenols	m/p-cresol							**2.0**	**17.8**
	p-ethylphenol	**0.5**							
Halogens	chloromethane		**8.0**		**1.6**		**9.0**		0.5
Methoxy phenols	guaiacol	**1.5**	**20.8**	**59.2**	**86.5**		0.9		
	4-vinylguaiacol	**44.4**							
	trans-isoeugenol	5.1	1.8						
	vanillin	2.3							
	syringol					**68.5**	**47.5**		
	p-ethylguaiacol	**3.2**	**5.8**						
	creosol	**2.4**	**1.9**				1.4	**65.9**	**70.0**
	(E)-4-(but-1-en-1-yl)guaiacol		1.6						
Monoaroma-tics	toluene							**2.4**	**3.7**
	benzene			1.1					
	2,5-dimethoxytoluene		2.0						
	p-cymene-2,5-diol		3.3						
	1,2,3-trimethoxybenzene					**1.0**	**2.1**		
Phenols	catechol				5.2				
	phenol			1.4	5.2		0.3		
	total volatiles quantified (wt.%)	59.5	47.2	61.6	99.2	69.5	62.9	70.4	92.6

+ traces in the MS chromatogram.
++ was detected with a peak area > 1%, but could not be quantified.

significantly lower than that of LG pyrolysis in salt B (ca. 94 wt%). Therefore, under the test conditions (350 °C, 0.4 MPa), the H_2 atmosphere favored non-condensable gases from LG in salt B instead of organic volatiles formation.

To the best of our knowledge, results on xylan (XYL) hydropyrolysis have not been published in the past. The main hydropyrolysis products from XYL were ketones (mainly hydroxyacetone, 1-hydroxy-2-butanone and 1,2-cyclopentadione), carboxylic acids (acetic acid and propanoic acid) and furfural. The H_2 atmosphere showed to enhance ring scission and rearrangement reactions of the XYL structure to favor hydroxyacetone formation, which was produced more than twice (ca. 9 wt%) compared to pyrolysis in a He atmosphere (ca. 4 wt%).

The production of furfural from XYL (through depolymerization, rearrangement and dehydration reactions) was less favorable under H_2 (ca. 4 wt%) compared to He (ca. 13 wt%). Surprisingly, under H_2 and with the addition of salt B, XYL produced more furfural (29 wt%) compared to He pyrolysis and with salt B added (23 wt%). Moreover, XYL hydropyrolysis with salt B also promoted the formation of other furanic compounds such as 2-methyl furan, furan and furfuryl alcohol. The formation of 2-methyl furan and furfuryl alcohol was solely derived from secondary hydropyrolysis reactions (i.e. not observed under XYL pyrolysis). Furfuryl alcohol was most likely formed as an intermediate product from furfural hydrogenation, and 2-methyl furan was produced from hydrogenolysis of furfuryl alcohol [5]. It was also observed that irrespective of the atmosphere used for LG, XYL or CEL, the presence of salt B promoted, to a certain extent, furfural decarbonylation leading to the production of furan. Also under H_2 atmosphere, XYL was the only hollocellulose derived-model compound which interacted with salt B when this was added and formed chloromethane (CH_3Cl).

With respect to cellulose (CEL), the type of hydropyrolysis products obtained from this model compound were comparable to those observed under He pyrolysis. However the total volatiles' yield from hydropyrolysis of pure CEL and CEL with salt B were respectively 21 wt% and 15 wt% lower than those from He pyrolysis. Regarding furfural (FF), Table 7 shows that pure FF hydropyrolysis caused partial hydrogenation to 2-methyl furan; whereas in the presence of salt B, this reaction was hindered which most likely occurred because of the diffusion barrier of the molten salts and therefore the limited contact between FF and the H_2 atmosphere.

3.2.2.2. Lignin derived model compounds. Table 8 shows that under H_2 atmosphere V-GUA was also, just like in regular pyrolysis, the most unstable lignin-derived model compound at 350 °C and 0.4 MPa, leading to the formation of other phenolics like *p*-ethylguaiacol, creosol and guaiacol. During V-GUA hydropyrolysis, guaiacol was formed (1.5 wt%) which could have resulted from the direct cracking of V-GUA (also forming ethylene) or alternatively, first by V-GUA demethylation to creosol (2.4 wt%) and then by creosol demethylation to guaiacol. Another observed reaction was the hydrogenation of the double bond in the side chain of V-GUA, which resulted in the formation of p-ethylguaiacol; this reaction was promoted by the H_2 atmosphere (3.2 wt%) compared to the He atmosphere (1.7 wt%) [37].

Just like in regular pyrolysis, V-GUA appeared to be very reactive during hydropyrolysis in the presence of salt B. The most favored reactions in the presence of salt B were the cracking of V-GUA to guaiacol (21 wt% ca.) on one side and the hydrogenation of V-GUA to p-ethyl guaiacol (6 wt%) on the other side. Importantly, with the addition of salt B, the yield of CH_3Cl from V-GUA hydropyrolysis (8 wt%) and from SYR hydropyrolysis (9 wt%) was much higher than from V-GUA pyrolysis (4 wt% ca.) or from SYR pyrolysis (3 wt% ca.)

As mentioned in the section for pyrolysis of model compounds (3.1.2), CH_3Cl can be formed from the reaction of methanol (from demethoxylation reactions of phenolics) and HCl (see eq. 1). In this case, HCl formation from hydrolysis of the chloride salts (see eq. 2) most likely occurred because of moisture uptake during the sample preparation of V-GUA and salt B, rather than from dehydration reactions (which do occur in lignocellulosic biomass pyrolysis). Nonetheless, in V-GUA and SYR hydropyrolysis with salt B, the source of HCl for CH_3Cl formation could also be the result from the interaction between the H_2 atmosphere and $ZnCl_2$ from salt B (see eq. 3).

$$ZnCl_2 + H_2O \rightarrow ZnO + 2HCl \quad (2)$$

$$ZnCl_2 + H_2 \rightarrow Zn + 2HCl \quad (3)$$

The production of HCl from either eq. 2 or eq. 3 have a similar thermodynamic probability for their occurrence (see Fig. S5 in the SI). The Gibbs free energy leading to HCl formation from eqs. 2 and 3 ($\Delta G = 0$) occurs at a temperature of around 9,001,150 °C, which could signal that neither hydrolysis nor hydrogenation of $ZnCl_2$ is thermodynamically favorable at the hydropyrolysis temperature used (350 °C). However, because in a chloride eutectic mixture ($ZnCl_2$:KCl:NaCl) the $ZnCl_2$ can hydrolyze (eq. 2) at pyrolysis temperatures as low as 350 °C (as shown in a previous study [21]), the reaction in eq. 3 is nevertheless expected to occur alongside the reactions in eqs. (1) and (2). This would at least explain the higher CH_3Cl yield from V-GUA and SYR hydropyrolysis compared to V-GUA and SYR pyrolysis under He atmosphere [11,21].

Table 8 clearly shows that the H_2 atmosphere promoted to a small extent hydrogenation of guaiacol (GUA), which provoked the scission of its C_{aryl}-OCH_3 bond and formed phenol (and traces of methanol as side-product). A further secondary hydrogenation reaction was observed, in which the C_{aryl}.OH bond from phenol was split, and formed benzene and water (although the latter was not measured in the GC–MS). Both reactions have been proposed as potential hydrodeoxygenation pathways from guaiacol [38]. The addition of salt B in GUA hydropyrolysis showed to promote the demethoxylation reaction of guaiacol (forming phenol) much more. Moreover, unlike with pure GUA hydropyrolysis, the presence of salt B additionally promoted GUA demethylation, which converted GUA into catechol and methane (although the latter was cannot measured in the GC–MS).

In the presence of the chloride salts, the yield obtained from syringol (SYR) hydropyrolysis was much lower than in their absence which can be explained simply by the promotion of demethoxylation reactions through catalysis by salt B. This is not observed in the case of pure SYR hydropyrolysis. The scission of the two C_{aryl}-OCH_3 bonds in SYR induced by salt B led to more methanol formation (compared to GUA, with only one C_{aryl}-OCH_3 bond) which further reacted with HCl (see eq. 2 or 3); this ultimately resulted in a higher CH_3Cl yield of 9 wt% as previously discussed. In addition, it was observed that the hydrogen atmosphere promoted the methylation of syringol to 1,2,3-trimethoxybenzene (1 wt %). In the presence of salt B, the 1,2,3-trimethoxybenzene yield was in fact higher (2.1 wt%). The conversion of syringol to 1,2,3-trimethoxybenzene has been previously observed in catalytic HDO studies with syringol as a side reaction, which has been attributed to its low active energy [39]. With regards to the hydropyrolysis of creosol (CRE), it was observed that demethoxylation occurred with and without the addition of salt B, which produced mainly p-cresol (but also m-cresol). However, salt B clearly enhanced the initial CRE volatilization and highly promoted its conversion to p-cresol. Moreover, hydrogenolysis of the –OH group in p/m-cresol resulted in the formation of toluene, with a yield slightly higher in the presence of salt B. An increase in the process temperature (which can be caused by the addition of salt B by enhancing the heat transfer) has been suggested to promote cresol hydrogenolysis [40].

A scheme of the main hydropyrolysis reactions of the lignin-derived model compounds is proposed in Fig. 7.

3.2.3. Effect of process conditions on the chemical groups' distribution

Fig. 8 and Fig. 9 show the changes in the chemical groups' distribution from PW and WS hydropyrolysis respectively, using chloride molten salts with different process variables (experiments numbered 1

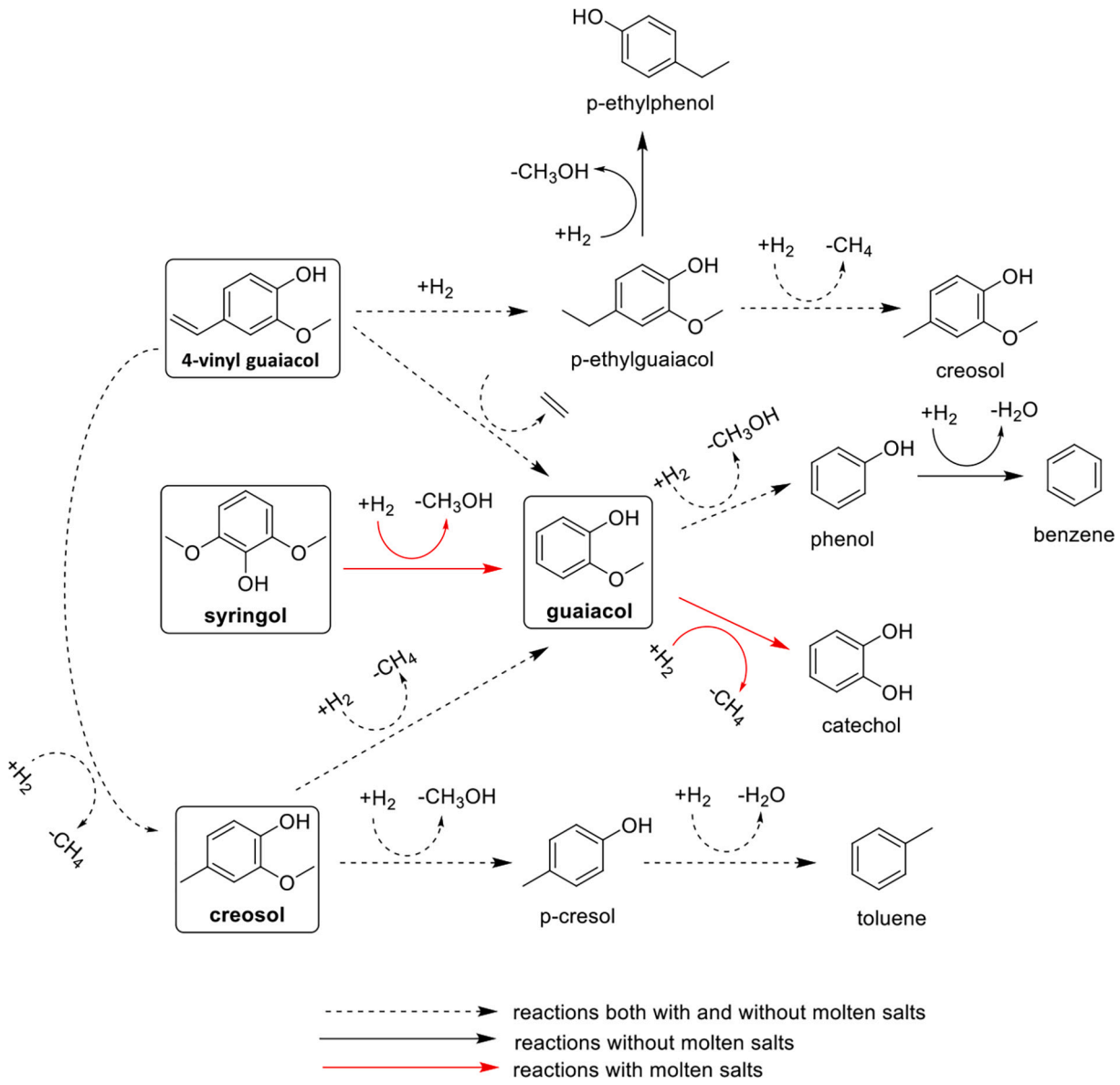

Fig. 7. Proposed hydropyrolysis reactions network for lignin-derived model compounds with and without chloride molten salts (salt B).

to 7). A reference test without molten salts ("/" in the figures) was also included and the list of individuals compounds included within each chemical group can be found in Table S5 from SI for PW and in Table S6 from SI for WS. Hereafter, first some noteworthy results from these supplementary information tables will be discussed.

As shown in sections 3.1 and 3.2, both the total yield of volatiles and the product distribution from pure PW and WS hydropyrolysis differed from that of PW and WS pyrolysis in helium (350 °C and 0.4 MPa). The total volatiles' yield, which were higher under He (ca. 55 wt% in PW and ca. 54 wt% in WS) than under H_2 (ca. 36 wt% in PW and ca. 45 wt% in WS), appeared to be influenced mainly by the yields of levoglucosan and acetic acid produced in each case. It has been demonstrated that under H_2 atmosphere, hydrocracking reactions of levoglucosan are promoted leading to the production of small oxygenates; this can explain the lower levoglucosan formation from PW hydropyrolysis (1.3 wt%, see Table S5) if compared to PW pyrolysis in helium (9.1 wt%, see Table S4) [17]. Also, the decrease in carboxylic acids (mainly acetic acid, see Tables S5 and S6) under H_2 can be explained because hydrogen deoxygenates acetic acid to acetaldehyde, a compound that was indeed observed exclusively under H_2. Moreover with respect to the changes in product distribution, it was observed that the yield of ketones from PW and WS hydropyrolysis (9.5 wt% and 12.9 wt% respectively, see Table S5 and S6) was higher than PW and WS pyrolysis (5.2 wt% and 9.5 wt% respectively, see Table S3). Hydroxyacetone was the main product from the ketones formed under hydrogen; the hydrogen atmosphere hence promoted the decomposition of anhydrosugars, which explains also the decrease in yield of levoglucosan. Finally, hydropyrolysis of both PW and WS induced a small formation of hydrocarbons (2,3-dimethylhexane and 2-butene in this study), which shows that H_2 atmosphere enhanced HDO reactions [17].

Now, hydropyrolysis of PW and WS with chloride molten salts under any process condition clearly showed that the prime group of compounds generated were furans, but also carboxylic acids and ketones. This was a clear difference with what was observed for pure PW and WS hydropyrolysis. These differences resemble the observations made for PW and WS pyrolysis with salt B (section 3.1.2). Apparently salt B catalyzed too the primary and secondary reactions of the hollocellulose fraction of PW and WS (forming furans predominantly), while it limited the pyrolysis of the lignin fraction within the lignocellulosic biomass (in particular the formation of methoxyphenols).

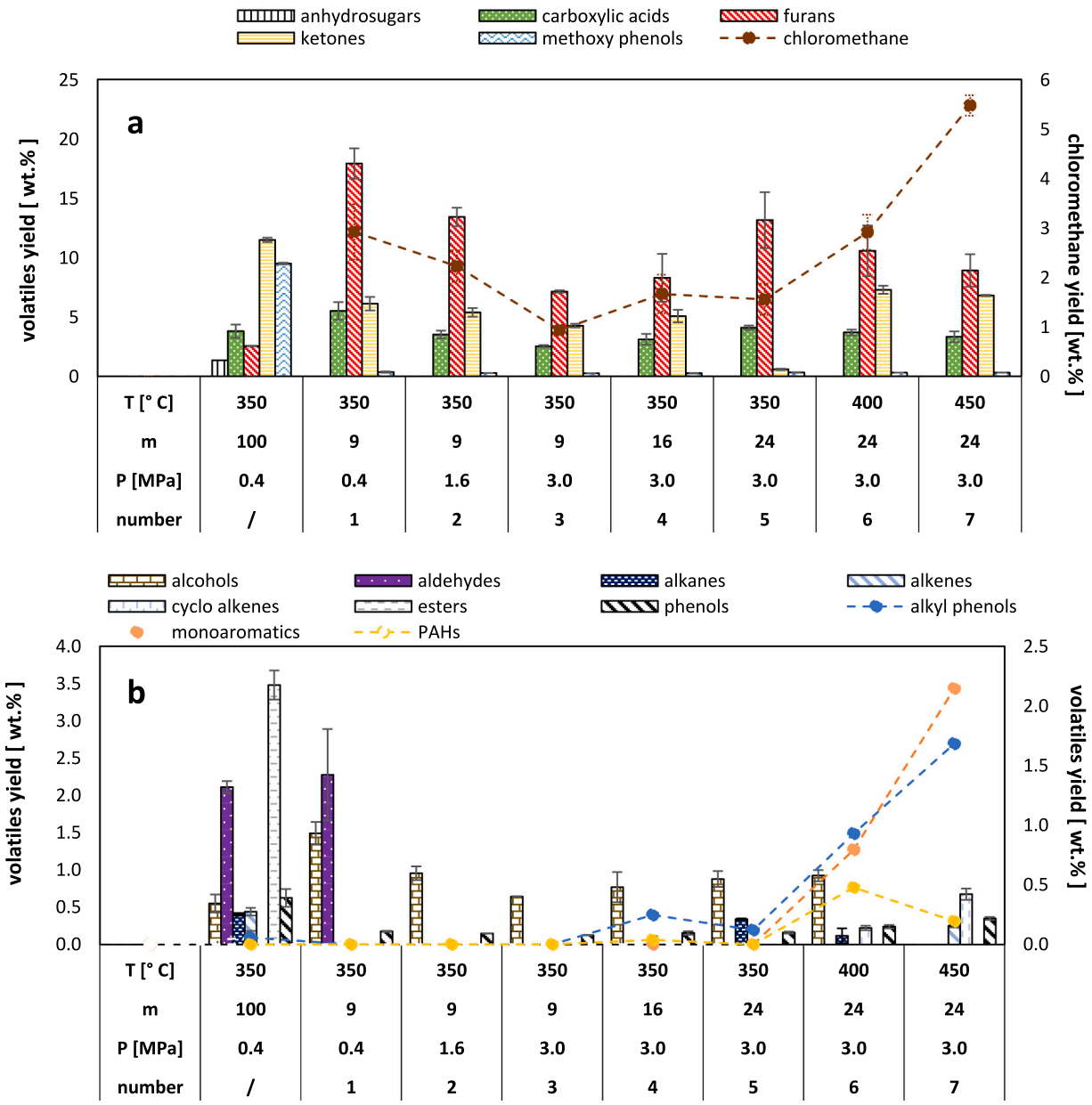

Fig. 8. Effect of process conditions (**T**: temperature, **m**: mass fraction of biomass in biomass-salt B mixture, **P**: pressure) in the chemical group distribution of pinewood hydropyrolysis using chloride molten salts (salt B – composed of $ZnCl_2$:KCl:NaCl in 44.3–41.9-13.8 mol%). Yields from bars are plotted on the left side y-axis, yields from dashed-lines are shown on the right y-axis. For the list of individuals compounds included within each group, the reader is referred to Table S4 from SI.

3.2.3.1. Pressure. From the two figures above it can be observed that the increase in hydropyrolysis pressure (from 0.4 MPa to 3.0 MPa) for both PW and WS in the presence of salt B, was detrimental for the yield of all the chemical groups. From all of these however, it was mainly the yield of furans that was affected. The increase in pressure impacted the yield of individual furans as follows: furfural > > 2-methyl furan > furan >5-methyl furfural > acetylfuran. In section 3.2.4, more details of the process variables' effect on the individual furans will be presented and discussed. Also noteworthy is that the carboxylic acids' yield (predominantly acetic acid) decreased with the increase in H_2 pressure, viz. from 5.5 wt% to 2.5 wt% in the case of PW (Fig. 8, a), and from 5.4 wt% to 2.9 wt% in the case of WS (Fig. 9, a). Moreover, the yield of ketones (mainly hydroxyacetone) decreased from 6.1 wt% to 4.3 wt% with PW (Fig. 8, a) and from 4.6 wt% to 0.3 wt% with WS (Fig. 9, a). Regarding the aldehydes (acetaldehyde mainly), these were only observed at 0.4 MPa H_2 pressure and were no longer detected at 1.6 MPa nor at 3.0 MPa (Fig. 8 and Fig. 9, b). Because of the overall decrease in the volatiles alongside the drop in CO_2 yield upon the increase in H_2 pressure (see Fig. S4), the combination of high-pressure and molten salts' together likely hinders the release of the volatiles. As a consequence char production is favored. Contrary to the effect of pressure, the effect of varying the quantities of biomass in the biomass-salt B mixture had a positive effect on the release of volatiles during molten salts hydropyrolysis as discussed next.

3.2.3.2. Biomass mass fraction in the biomass-salt B mixture. The increase of biomass mass fraction in the biomass-salt B mixture (i.e. less molten salts) in PW high-pressure hydropyrolysis with salt B improved the release of volatiles (experiment number 3 to 5 in Fig. 8). For instance, Fig. 8-a shows an increase in volatiles' yield for the furans above all (ca. 7 wt% to 13 wt%) and for the carboxylic acids (2.5 wt% to

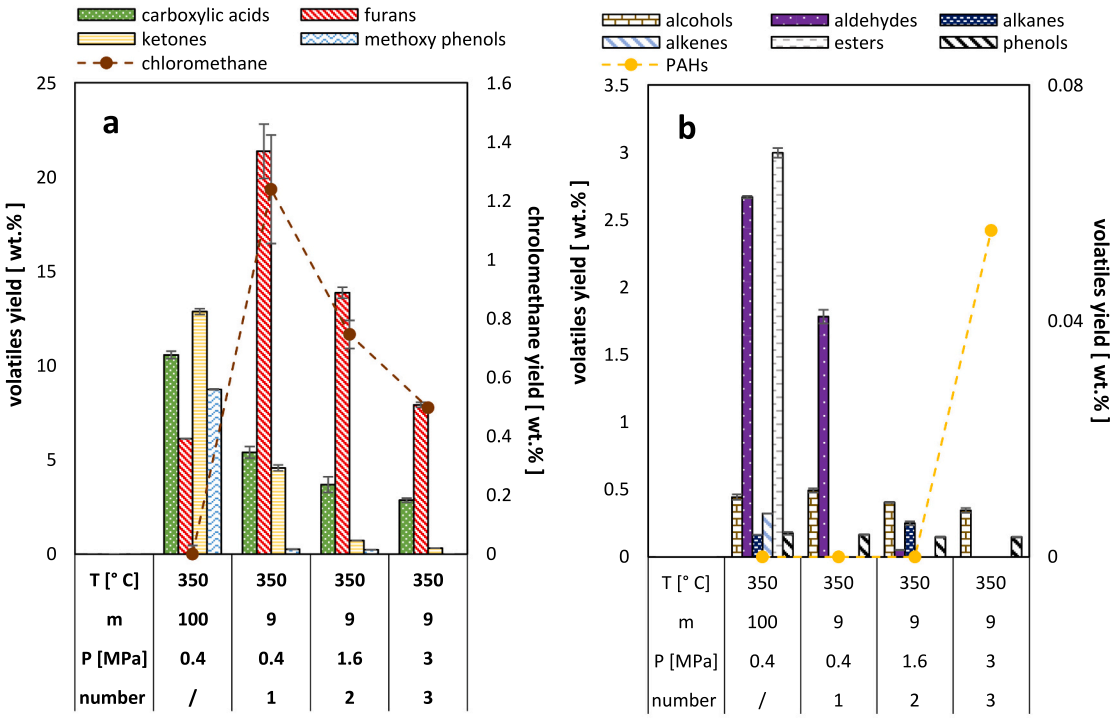

Fig. 9. Effect of varying pressure in the chemical group distribution of wheat straw hydropyrolysis using chloride molten salts (salt B – composed of $ZnCl_2$:KCl:NaCl in 44.3–41.9-13.8 mol%). Yields from bars are read in the left y-axis, yields from dashed-lines are read on the right y-axis. For the list of individuals compounds included within each group, the reader is referred to Table S5 from SI.

4.1 wt%). Moreover, the formation of alkyl phenols (m/o cresol) shown in Table S5 was observed because of the reduced quantities of molten salts used. In this case, creosol which is formed from pure PW hydropyrolysis (0.9 wt%), was demethoxylated in the presence of salt B and formed m/o cresol (as indicated in Fig. 7). Another point regarding the increase of biomass mass fraction in the biomass-salt B mixture was that this variable did not lowered the CH_3Cl yield as it was expected. On the contrary, the CH_3Cl yield slightly increased when the PW mass fraction in the biomass-salt B mixture was increased from 9 wt% to 16 wt% and then stabilized at 24 wt% (Fig. 8, a). It is therefore possible that even with less quantities of molten salts used (i.e. 84 wt% or 76 wt% compared to 91 wt%), the salts can still react with the more available PW mass fraction and formed slightly a higher yield of CH_3Cl. Nonetheless, the particular advantage of high-pressure and a high-biomass mass fraction in PW hydropyrolysis with salt B was that the CH_3Cl yield was almost 50% lower than at low H_2 pressure (0.4 MPa) while the production of furans was only slightly decreased.

3.2.3.3. Temperature. With respect to the increase in temperature from 350 to 450 °C for hydropyrolysis of PW with salt B (experiment number 5 to 7), it is fair to say that there were advantages and disadvantages when considering the yields obtained. One of the downsides with the temperature increase was that the yield of furans dropped from ca. 13 wt % to 7 wt%, most likely due to enhanced decarbonylation of furfural to form furan (described in section 3.2.4) and CO at higher temperatures and in the presence of H_2 [41]. Also, the combination of high temperature and high pressure conditions contributed in the formation of PAHs. PAHs from hydropyrolysis of lignocellulosic biomass in salt B could come from the lignin fraction (forming 3-ring PAHs) or from the cellulose/xylan fraction (forming 2-ring PAHs) [18,42]. Ring growth via Diels-Alder cycloaddition reaction pathways in combination with hydrogen abstraction/C_2H_2 addition have been shown to be a feasible mechanism in the formation of PAHs [42]. Moreover, the CH_3Cl formation (eq. 1) was promoted at the higher hydropyrolysis temperatures, leading to an important increase of its yield from 1.5 wt% (at 350 °C) to 5.5 wt% (at 450 °C) as shown in Fig. 8, a. It is likely that at a temperature > 350 °C, more methanol is available to react with HCl and form CH_3Cl. A higher yield of methanol can be caused by multiple demethoxylation of the methoxyphenols obtained from PW (like 4-vinyl guaiacol, guaiacol and creosol), which have been demonstrated to be catalyzed by salt B in Table 8. In spite of the formation of methoxyphenols not being favored in the presence of salt B (experiment number 1 to 5 in Fig. 8, a), it may be that with the increase in temperature (350 °C → 450 °C), the initial conversion of the lignin fraction within PW was improved towards the formation of methoxy phenols, and instantly demethoxylated [18].

Now, some of the benefits of the temperature increase were that the non-methoxyphenols or alkyl phenols' yield increased at 400 °C (up to 0.9 wt%) and then at 450 °C (up to 1.7 wt%) as observed in Fig. 8, b; these consisted of *m/p/o* cresol, but also dimethylphenol isomers and ethylphenol isomers. These data support the observations from Patwardhan et al. (2011) on the temperature effect in lignin pyrolysis and also support the previous hypothesis of an enhanced demethoxylation of methoxyphenols at 400–450 °C [43]. For instance, one potential route for ethylphenol formation is the hydrogenation/demethoxylation of 4-vinyl guaiacol, as shown in Fig. 7. Another benefit of the temperature increase was the rising yield of monoaromatics which increased from 0.1 wt% at 350 °C to 2.1 wt% at 450 °C (Fig. 8, b); they consisted of toluene, pentamethylbenzene, 1-ethyl-2,4,5-trimethylbenzene, xylene and benzene. An increase in pyrolysis temperature has shown to improve the yield in benzene from lignin intermediates [44]. Moreover, these results also support the work of Wang et al. (2022), in which the production of monocyclic aromatics from lignin hydropyrolysis was enhanced at 3.0 MPa H_2 pressure and 500 °C, suggesting that the formation of monoaromatics occurred by the substitution of phenolic OH groups by hydrogen radicals (from hydrogen gas) and methyl groups were formed by the cleavage of O-CH_3 bonds [18]. A route towards the production of monoaromatics can also be through Diels-Alder reactions with cellulose pyrolysis products (such as 3-methyl furan); it has been demonstrated that this reaction was promoted under a high temperature

and high H_2 pressure [17].

3.2.4. Effect of process conditions on furanics

This subsection focuses on the furanics solely and the production of MF because of its interest as a renewable fuel additive. As previously mentioned, the effect of the three studied variables (pressure, mass fraction of biomass in biomass-salt B mixture and temperature) was further assessed on the individual furanic compounds obtained from hydropyrolysis of lignocellulosic biomass with salt B. The list of furans consisted of: furfural (FF), 2-methyl furan (MF), 2,5-dimethyl furan (DMF), 2-acetylfuran (ACF), furan (FUR), 5-methyl furfural (MFF) and furfuryl alcohol (FA). Fig. 10 shows the effect of pressure, biomass mass fraction in biomass-salt B mixture and temperature on the yield of furans obtained in molten salts hydropyrolysis of pinewood (PW). Fig. 11 only shows the effect of pressure in molten salts hydropyrolysis of wheat straw (WS).

Variation in the furans yields were clearly observed, especially regarding FF and MF from both PW and WS (Fig. 10 and Fig. 11, a). This may be caused by the complexity in preparing a homogenous mixture of biomass and salt B. The high hygroscopicity of salt B can cause salts residues to adhere to the mixing spatula, be then partially removed and ultimately limit the catalytic activity of salt B during biomass hydropyrolysis. Another explanation may be that, unlike with He (inert atmosphere), the H_2 atmosphere promotes hydrogenation reactions which

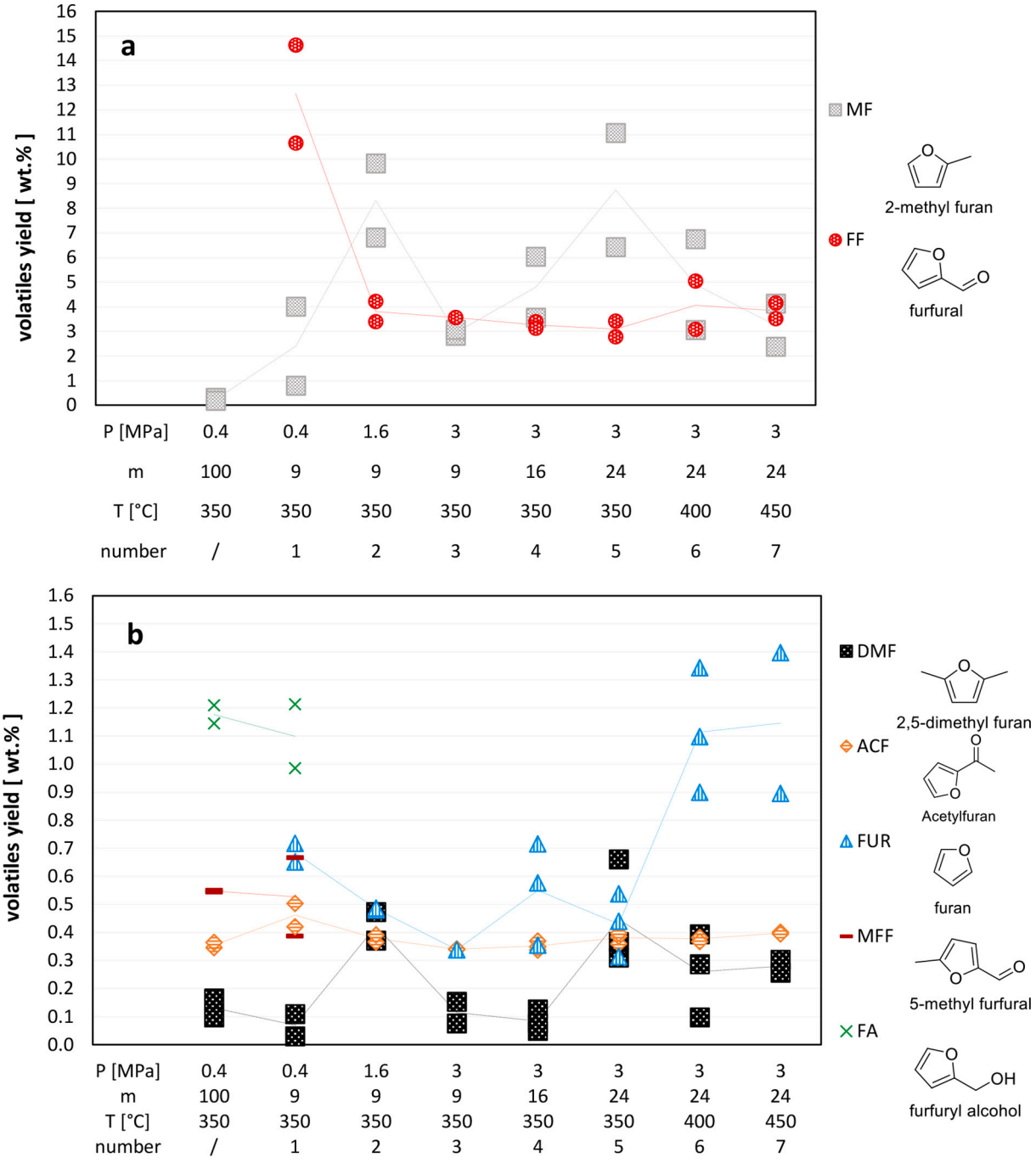

Fig. 10. Pinewood hydropyrolysis: effect of multiple process conditions (**P**: pressure, **m**: biomass mass fraction in biomass-salt B mixture and **T**: temperature) in FF, MF, DMF, ACF, FUR, MFF and FA production using a mixture of chloride molten salts (salt B) which is composed of $ZnCl_2$:KCl:NaCl in the ratio of 44.3–41.9-13.8 mol%.

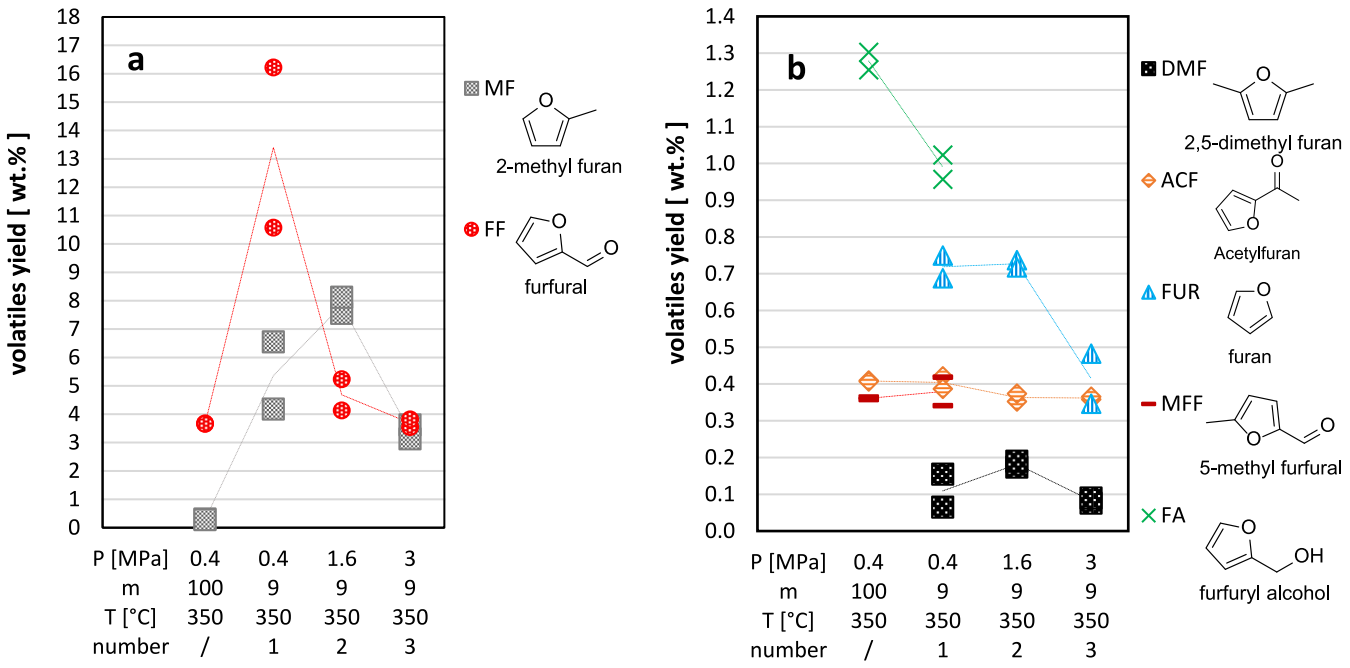

Fig. 11. Wheat straw hydropyrolysis: effect of pressure in MF, FF, DMF, ACF, FUR, MFF and FA production using a mixture of chloride molten salts (salt B) which is composed of $ZnCl_2$:KCl:NaCl in the ratio of 44.3–41.9-13.8 mol%.

makes furfural (the main furanic compound catalyzed by salt B) unstable and reactive. The proposed mechanisms in the production and conversion of furans from PW and WS hydropyrolysis with salt B are depicted in Fig. 12.

In the hydropyrolysis studies of model compounds (section 3.2.2) it was shown that furfural can be formed from the holocellulose fraction of PW and WS via two routes. Through a first route (R-1 in Fig. 12), furfural can be formed through dehydroxymethylation of HMF, with formaldehyde as a by-product. The production of HMF itself can occur by direct ring opening/cyclization reactions of aldohexoses (D-glucose). But it can also be formed as a secondary decomposition product of levoglucosan [28]. Secondary decomposition of levoglucosan to HMF though, was more likely to occur in PW, because only in this case levoglucosan was produced (1.3 wt%). A second route for furfural turnout (R-2) was through depolymerization, rearrangement and dehydration reactions of aldopentoses stemming from the hemicellulose fraction (e.g. d-xylose).

The conversion of FF to MF is of particular interest in this study because of MF's potential as a fuel additive [5]. MF was formed from pure PW and WS hydropyrolysis at 350 °C in small quantities (0.2 wt% and 0.3 wt% respectively, shown in Fig. 10, a and Fig. 11, a), however its yield increased with the addition of salt B depending on the process conditions employed. In H_2 atmosphere, FF undergoes hydrogenation

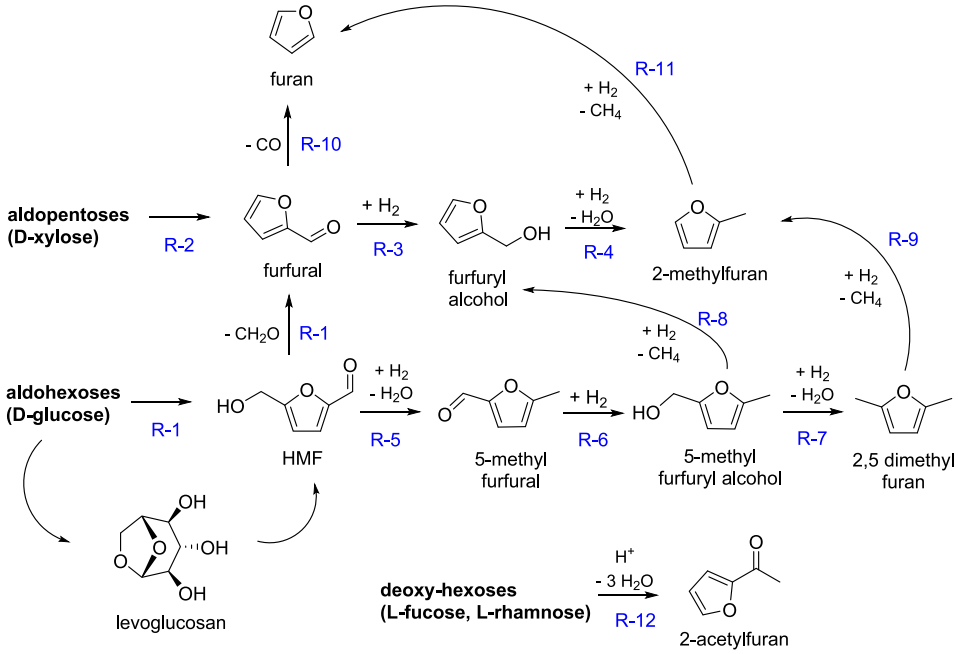

Fig. 12. Proposed reaction pathways of furanic compounds during lignocellulosic biomass hydropyrolysis with a mixture of chloride molten salts (salt B). [28,29,41,45,46].

(R-3) which produces furfuryl alcohol (FA), as shown in Fig. 10, b and Fig. 11, b. Consequently, hydrogenolysis of FA (R-4) leads to the formation of MF. Because FF production was only observed from WS hydropyrolysis and not from PW, it is possible to hypothesize that reaction pathways leading to MF's formation differed between the biomasses. As explained earlier in section 3.1.3, the higher ash content in WS (compared to PW) can explain the promoted dehydration reactions from the holocellulose fraction leading to the formation of ca. 3.7 wt% furfural (and no levoglucosan); therefore MF from WS hydropyrolysis could be formed from FF via R-3 and R-4. Nonetheless, another plausible reaction mechanism leading to MF production could be through a series of reactions starting off from HMF, in which 5-methyl furfural (MFF) and 2,5-dimethyl furan (DMF) are intermediates, both found as hydropyrolysis products from WS and PW (Fig. 10, b and Fig. 11, b). The series of reactions consist of: 1) hydrogenolysis of HMF (R-5) which resulted in MFF, 2) hydrogenation of MFF to 5-methyl furfuryl alcohol (R-6), 3) hydrogenolysis of 5-methyl furfuryl alcohol to DMF (R-7) and 4) hydrogenolysis of DMF to MF (R-9). Alternatively to this route, 5-methyl furfuryl alcohol can also react with H_2 and form FA (R-8) and from there, FA becomes the intermediate to MF (R-4).

In the presence of salt B and at low H_2 pressure (0.4 MPa), the main furanic compound produced was furfural in both PW and WS, with an average yield ranging from ca. 12.6 wt% to 13.4 wt% respectively (Fig. 10 and Fig. 11, a). Under these conditions, MF could still have been produced via different routes. Because FA was encountered in both PW and WS (ca. 1 wt%, shown in Fig. 10 and Fig. 11, b), the production of MF could have occurred via R-3 followed by R-4 starting off from FF. Moreover, both MFF and DMF were also intermediates found in both biomasses, hence MF was potentially formed too via R-5 - > R-6 - > R-7 - > R-9.

Upon the increase in H_2 pressure from 0.4 MPa to 1.6 MPa and 3.0 MPa, with the exception of DMF, the intermediates FA and MFF were no longer produced from neither of the biomasses (see Fig. 10 and Fig. 11, b). Given DMF's formation throughout the rest of the process variables tested (experiment number 2 to 7) and its resembling trend in yield to MF (both in WS and PW, Fig. 10 and Fig. 11, a), it is possible to hypothesize that at pressure > 1.6 MPa, MF formation occurred via R-9 rather than R-4. The increase in pressure from 0.4 MPa to 1.6 MPa improved the MF yields from PW and WS hydropyrolysis with salt B; the average MF yield increased in PW from 2.4 wt% to 8.3 wt% and in WS from 5.4 wt% to 7.8 wt%. At higher pressures (3.0 MPa), the MF yield dropped in both cases to <4 wt%.

Concerning the increase of biomass mass fraction in biomass-salt B mixture from 9 wt% to 24 wt%, this appeared to be favorable for the MF's formation, reaching in average 8.7 wt% from PW (Fig. 10, a). On the other hand, the increase in temperature from 350 °C to 450 °C was not beneficial for MF's production because it reduced its yield to more than half.

Furan (FUR) and acetylfuran (ACF) were also furans encountered from PW and WS hydropyrolysis (Fig. 10, b and Fig. 11, b). FUR was formed from PW and WS hydropyrolysis only in the presence of salt B, as the result of FF decarbonylation reactions or MF demethylation reactions (R-10 and R-11 in Fig. 12). At high temperatures though (~ 600 °C), it cannot be excluded that furan is formed directly from levoglucosan without furfural as an intermediate [47]. The yield of FUR decreased with increasing pressure, slightly improved with the increase in biomass mass fraction in biomass-salt B mixture and was enhanced by the temperature increase, reaching a maximum average of 1.1 wt% (most likely via R-11). With respect to ACF, this was formed from hydropyrolysis of both biomasses with and without salt B and was unaltered by the tested process variables. ACF can be separately formed from dehydration reactions of deoxy-hexoses (R-12).

3.2.5. Optimal process conditions for molten salts hydropyrolysis

With the exception of temperature, both the increase in pressure and mass fraction of biomass in biomass-salt B mixture had a positive influence on molten salts hydropyrolysis of lignocellulosic biomass. This is concluded based on the yield of MF obtained, which shows the extent of promoted hydrogenation, hydrodeoxygenation and demethylation reactions of furan-ring compounds (as shown in Fig. 12). From this point of view, two alternatives can be considered optimal for MF formation: 1) H_2 pressure of 1.6 MPa and biomass mass fraction in biomass-salt B mixture of 0.09 (MF yield: ca. 8.3 wt% from PW and 8.1 wt% from WS) and, 2) H_2 pressure of 3.0 MPa and biomass mass fraction in biomass-salt B mixture of 0.24 (MF yield: 8.7 wt% from PW). However, further research is required to determine whether the combination of H_2 pressure of 1.6 MPa and a biomass mass fraction in biomass-salt B mixture of 0.24 (or higher) could result in even higher MF's yields.

3.2.6. Individual catalytic effect the constituents chloride salts in salt B

So far, the focus of section 3 has been on the effect of different process variables in hydropyrolysis of lignocellulosic biomasses with chloride molten salts (salt B). This last subsection will deal with the individual chloride salts used ($ZnCl_2$, KCl and NaCl) and their separated catalytic effect in pinewood (PW) hydropyrolysis with salt B. Fig. 13 shows a series of chromatograms that compare hydropyrolysis of pure PW, PW with salt B and PW with each chloride salt.

Clearly, the selective portfolio of products (mainly furfural and acetic acid) that has been observed from PW and salt B hydropyrolysis, was the result of the catalytic activity of $ZnCl_2$ in the eutectic mixture (chromatograms in green). It has been previously reported that $ZnCl_2$, which is a Lewis acid, promoted depolymerization and dehydration of hollocellulose in biomass to form furfural [48]. This was also visible from the chromatogram obtained from pinewood hydropyrolysis with $ZnCl_2$, where distinctly a furfural peak (no. 5 in Fig. 13) was observed. The hydropyrolysis chromatograms from PW with KCl and PW with NaCl resembled each other, as well as the one of pure PW (chromatograms in blue). It suggests that these salts did not contribute to the observed catalytic effect in PW hydropyrolysis with salt B.

Although this study has been highly focused on the catalytic properties of chloride molten salts, it is important to recollect the earlier claim that molten salts also act as a heat carrier during thermal conversion of lignocellulosic biomass. The eutectic salt mixture (salt B) also has a much lower melting point (204 °C) than the individual salts which ensures that salt B is in a liquid state before any biomass thermal degradation reaction takes place upon heating [21]. The latter was evidenced by observing a higher total volatiles yield from PW in the molten salts (salt B) compared to any of the yields attained from PW with the individuals chloride salts (Table 9).

4. Conclusions

Results of analytical micro-scale pyrolysis and hydropyrolysis (py-GC–MS/FID) of lignocellulosic biomass like pinewood and wheat straw and model compounds derived from the hollocellulose and lignin fraction were compared in the presence and absence of chloride molten salts. The chloride molten salts consisted of a $ZnCl_2$:KCl:NaCl eutectic mixture (named salt B). Under H_2 and in the presence of salt B, the effect of 3 process variables was assessed with respect to the total yield and quality of detectable volatiles. These variables were 1) pressure, 2) the biomass mass fraction in the biomass-salt B mixture and 3) temperature.

The increase in biomass mass fraction from 0.05 to 0.09 (i.e. less salts) improved the release of pyrolysis volatiles, yielding ca. 53 wt% volatiles from wheat straw and to 55 wt% volatiles from pinewood. The carbon distribution of the pyrolysis volatiles with salt B mainly consisted C_5 compounds (ca. 31 wt%) and C_2 compounds (15 to 18 wt%), where the main C_2 and C_5 compounds were acetic acid and furfural respectively. The analysis of the model compounds both under He and H_2 showed that: 1) salt B highly promoted primary and secondary reactions of hollocellulose leading primarily to the formation of furfural and acetic acid through various possible mechanisms and 2) regarding the lignin fraction, salt B promoted demethoxylation reactions which formed

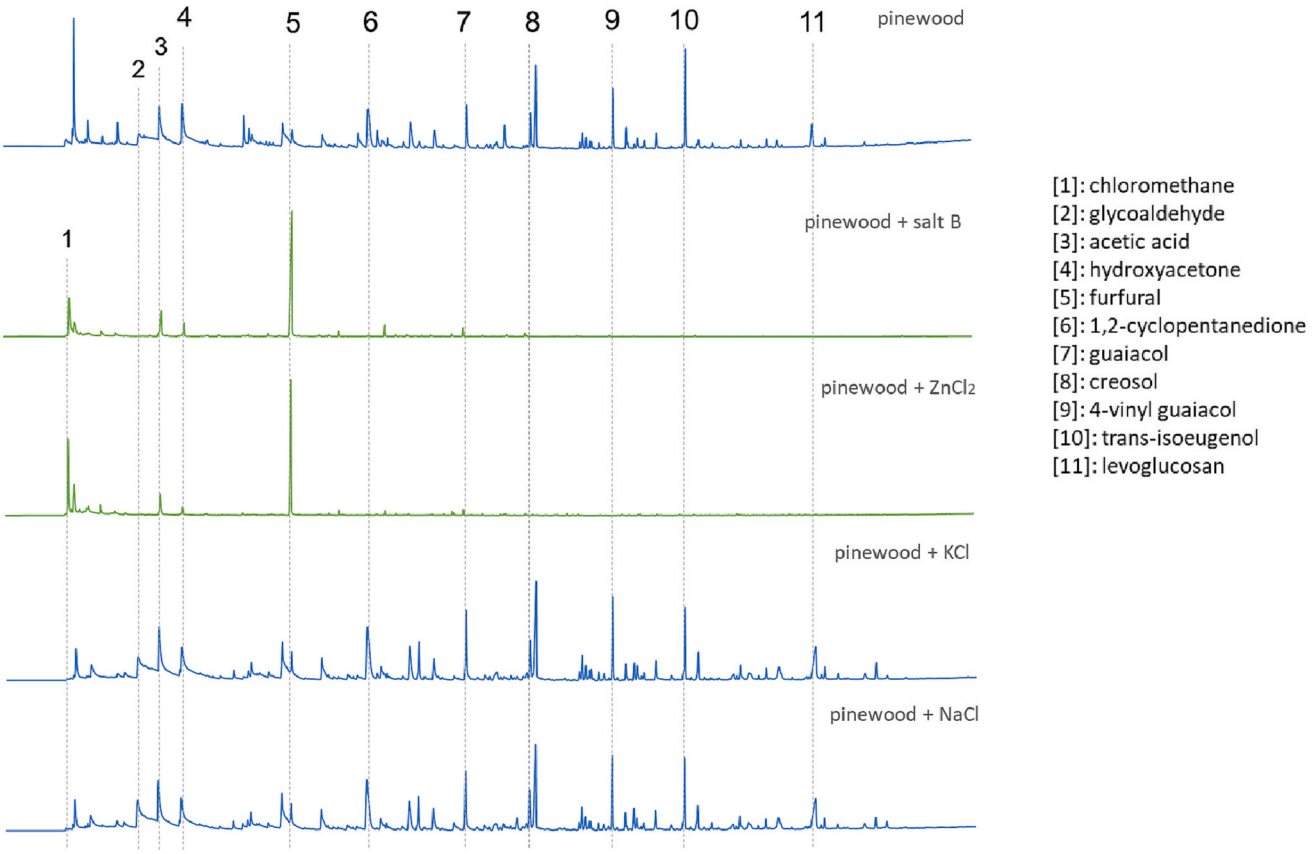

Fig. 13. Effect of individual chloride salts of salt B on hydropyrolysis products from pinewood; performed at 0.4 MPa, 350 °C and 40 wt% biomass mass fraction in biomass-salt B mixture; salt B is composed of $ZnCl_2$:KCl:NaCl in the ratio of 44.3–41.9-13.8 mol%.

Table 9
Total volatiles yield (wt%) from pinewood hydropyrolysis as (1) pure, (2) with the eutectic mixture salt B and (3) with its individual chloride salts. Performed at 0.4 MPa, 40 wt% biomass mass fraction in biomass-salt B mixture and 350 °C.

	total volatiles yield [wt%]*
pure PW	36.9
PW with salt B	24.7
PW with $ZnCl_2$	18.1
PW with KCl	21.2
PW with NaCl	21.7

* excludes chloromethane yield.

mainly guaiacol and phenol, and chloromethane as by-product. The yield of chloromethane was higher when the lignocellulosic biomass and salt B were hydropyrolyzed rather than pyrolyzed, most probably because an interaction between H_2 and $ZnCl_2$ occurred. This reaction produces additional HCl, inevitably occurring from the salts hydrolysis, and reacts with methanol (from demethoxylation reactions of lignin-derived phenolics) to form chloromethane. Importantly, the quality of furan-ring compounds (predominant in the presence of salt B) was improved under H_2 atmosphere because it promoted hydrogenation, hydrodeoxygenation and demethylation reactions and ultimately increased the production of 2-methyl furan, a prospective fuel additive. The main proposed reaction pathway in MF production was through furfural hydrogenation to furfuryl alcohol, followed by hydrodeoxygenation of the latter to 2-methylfuran.

The optimal conditions found for the production of 2-methyl furan from lignocellulosic biomass hydropyrolysis with salt B were either at 1.6 MPa (biomass mass fraction of 0.09) or at 3.0 MPa (with a higher biomass mass fraction of 0.24), both at a temperature of 350 °C. Under these optimal conditions, MF yields were 8.2 and 8.7 wt% respectively. Higher temperatures (450 °C) were not favorable for the production of 2-methylfuran and instead promoted furfural decarbonylation to furan. Relevantly, it was demonstrated that $ZnCl_2$ was the sole catalytically active salt within salt B. Nevertheless, the benefit of employing salt B (and not just $ZnCl_2$) during biomass hydropyrolysis was observed from the attained higher volatiles yield compared to those obtained with all 3 of the individual salts. This showed the ability of the molten salts to act as a heat carrier too.

CRediT authorship contribution statement

Adriana Estrada Leon: Investigation, Writing – original draft, Formal analysis. **Racchana Ramamurthy:** Formal analysis. **Stef Ghysels:** Writing – review & editing. **Sepideh Niazi:** Investigation, Validation. **Wolter Prins:** Writing – review & editing, Supervision. **Frederik Ronsse:** Writing – review & editing, Supervision, Project administration, Resources.

Declaration of Competing Interest

The authors declare the following financial interests/personal relationships which may be considered as potential competing interests:

Adriana Estrada Leon reports financial support was provided by European Commission. Racchana Ramamurthy reports financial support was provided by European Commission. Sepideh Niazi reports financial support was provided by European Commission. Wolter Prins reports financial support was provided by European Commission. Frederik Ronsse reports financial support was provided by European Commission.

Data availability

Data will be made available on request.

Acknowledgments

This project has received funding from the European Union's Horizon 2020 research and innovation programme under grant agreement N° 764089. The authors thank Leon Rohrbach and Kris Steenwegen for their technical support. Also, the authors would like to thank the ABC-Salt consortium.

Appendix A. Supplementary data

Supplementary data to this article can be found online at https://doi.org/10.1016/j.fuproc.2023.107917.

References

[1] European Environment Agency, Fuel Quality in the EU in 2016 - Fuel Quality Monitoring under the Fuel Quality Directive, 2018.
[2] R. Pacheco, C. Silva, Global warming potential of biomass-to-ethanol: review and sensitivity analysis through a case study, Energies. 12 (2019), https://doi.org/10.3390/en12132535.
[3] R. GRAY, Why Raising the Alcohol Content of Europe's Fuels Could Reduce Carbon Emissions, EU Res. Innov. Mag, 2020 https://ec.europa.eu/research-and-innovation/en/horizon-magazine/why-raising-alcohol-content-europes-fuels-could-reduce-carbon-emissions (accessed January 2, 2023).
[4] E4tech, E20 Supply and Demand Study - for ePURE, 2019, p. 21.
[5] A. Tuan Hoang, V. Viet Pham, 2-Methylfuran (MF) as a potential biofuel: a thorough review on the production pathway from biomass, combustion progress, and application in engines, Renew, Sustain. Energy Rev. 148 (2021), 111265, https://doi.org/10.1016/j.rser.2021.111265.
[6] Y. Wang, D. Zhao, D. Rodríguez-Padrón, C. Len, Recent advances in catalytic hydrogenation of furfural, Catalysts. 9 (2019), https://doi.org/10.3390/catal9100796.
[7] M.J. Taylor, L. Jiang, J. Reichert, A.C. Papageorgiou, S.K. Beaumont, K. Wilson, A. F. Lee, J.V. Barth, G. Kyriakou, Catalytic hydrogenation and hydrodeoxygenation of furfural over Pt(111): a model system for the rational design and operation of practical biomass conversion catalysts, J. Phys. Chem. C 121 (2017) 8490–8497, https://doi.org/10.1021/acs.jpcc.7b01744.
[8] K. Zhou, J. Chen, Y. Cheng, Z. Chen, S. Kang, Z. Cai, Y. Xu, J. Wei, Enhanced catalytic transfer hydrogenation of biomass-based furfural into 2-methylfuran over multifunctional Cu-Re bimetallic catalysts, ACS Sustain. Chem. Eng. 8 (2020) 16624–16636, https://doi.org/10.1021/acssuschemeng.0c06026.
[9] W. Burnette, Production of 2-Methylfuran by Vapor- Phase Hy rsgenation of Furfural, 40 (n.d.) 502–505.
[10] F. Deng, A.S. Amarasekara, Catalytic upgrading of biomass derived furans, Ind. Crop. Prod. 159 (2021), 113055, https://doi.org/10.1016/j.indcrop.2020.113055.
[11] A. Estrada Leon, M. Pala, H.J. Heeres, W. Prins, F. Ronsse, Micro-pyrolysis of various lignocellulosic biomasses in molten chloride salts, J. Anal. Appl. Pyrolysis 168 (2022), 105739, https://doi.org/10.1016/j.jaap.2022.105739.
[12] R. Datta, J. Dittami, Molten Salt Pyrolysis for Bio-Oil and Chemicals. WO 2017/007798 Al. https://patentscope.wipo.int/search/en/detail.jsf?docId=WO2017007798, 2017.
[13] H.S. Nygård, E. Olsen, Review of thermal processing of biomass and waste in molten salts for production of renewable fuels and chemicals, Int. J. Low-Carbon Technol. 7 (2012) 318–324, https://doi.org/10.1093/ijlct/ctr045.
[14] C. Di Blasi, C. Branca, Temperatures of wood particles in a hot sand bed fluidized by nitrogen, Energy Fuel 17 (2003) 247–254, https://doi.org/10.1021/ef020146e.
[15] H.S. Nygård, F. Danielsen, E. Olsen, Thermal history of wood particles in molten salt pyrolysis, Energy Fuel 26 (2012) 6419–6425, https://doi.org/10.1021/ef301121j.
[16] F.L.P. Resende, Recent advances on fast hydropyrolysis of biomass, Catal. Today 269 (2016) 148–155, https://doi.org/10.1016/j.cattod.2016.01.004.
[17] T. Li, K. Miao, Z. Zhao, Y. Li, H. Wang, A. Watanabe, N. Teramae, K. Wang, Understanding cellulose pyrolysis under hydrogen atmosphere, Energy Convers. Manag. 254 (2022), 115195, https://doi.org/10.1016/j.enconman.2021.115195.
[18] H. Wang, T. Li, J. Su, K. Miao, K. Wang, Noncatalytic hydropyrolysis of lignin in a high pressure micro-pyrolyzer, Fuel Process. Technol. 233 (2022), https://doi.org/10.1016/j.fuproc.2022.107289.
[19] S. Gundekari, S.K. Karmee, Catalytic hydropyrolysis of lignin for the preparation of cyclic hydrocarbon-based biofuels, Catalysts. 12 (2022) 1–24, https://doi.org/10.3390/catal12121651.
[20] M.Z. Stummann, M. Høj, A.B. Hansen, B. Davidsen, P. Wiwel, J. Gabrielsen, P. A. Jensen, A.D. Jensen, New insights into the effect of pressure on catalytic hydropyrolysis of biomass, Fuel Process. Technol. 193 (2019) 392–403, https://doi.org/10.1016/j.fuproc.2019.05.037.
[21] S. Niazi, E. Olsen, H.S. Nygård, Hydrolysis of eutectic compositions in the ZnCl2: KCl:NaCl ternary system and effect of adding ZnO, J. Mol. Liq. 317 (2020), 114069, https://doi.org/10.1016/j.molliq.2020.114069.
[22] J.T. Scanlon, D.E. Willis, Calculation of flame ionization detector relative response factors using the effective carbon number concept, J. Chromatogr. Sci. 23 (1985) 333–340, https://doi.org/10.1093/chromsci/23.8.333.
[23] S. Niazi, Experimental and Theoretical Evaluation of Thermodynamic Properties of Low Melting Chlorides Suitable for Liquefaction of Biomass, Norwegian University of Life Sciences (NMBU), 2022.
[24] P.R. Patwardhan, R.C. Brown, B.H. Shanks, Product distribution from the fast pyrolysis of hemicellulose, ChemSusChem. 4 (2011) 636–643, https://doi.org/10.1002/cssc.201000425.
[25] B. Sridharan, H.C. Genuino, D. Jardan, E. Wilbers, H.H. Van De Bovenkamp, J.G. M. Winkelman, R.H. Venderbosch, H.J. Heeres, Novel route to produce hydrocarbons from woody biomass using molten salts, Energy Fuel 36 (2022) 12628–12640, https://doi.org/10.1021/acs.energyfuels.2c02044.
[26] R.J.M. Westerhof, S.R.G. Oudenhoven, P.S. Marathe, M. Engelen, M. Garcia-Perez, Z. Wang, S.R.A. Kersten, The interplay between chemistry and heat/mass transfer during the fast pyrolysis of cellulose, React. Chem. Eng. 1 (2016) 555–566, https://doi.org/10.1039/c6re00100a.
[27] P.R. Patwardhan, D.L. Dalluge, B.H. Shanks, R.C. Brown, Distinguishing primary and secondary reactions of cellulose pyrolysis, Bioresour. Technol. 102 (2011) 5265–5269, https://doi.org/10.1016/j.biortech.2011.02.018.
[28] D.K. Shen, S. Gu, The mechanism for thermal decomposition of cellulose and its main products, Bioresour. Technol. 100 (2009) 6496–6504, https://doi.org/10.1016/j.biortech.2009.06.095.
[29] S.T. Moe, G. Marcotullio, M.T. Opedal, R. Brusletto, Formation of 5-methylfurfural and 2-acetylfuran from lignocellulosic biomass and by Cr3+−catalyzed dehydration of 6-deoxyhexoses, Carbohydr. Res. 522 (2022) 1–7, https://doi.org/10.1016/j.carres.2022.108672.
[30] V. Maliekkal, S. Maduskar, D.J. Saxon, M. Nasiri, T.M. Reineke, M. Neurock, P. Dauenhauer, Activation of cellulose via cooperative hydroxyl-catalyzed transglycosylation of glycosidic bonds, ACS Catal. 9 (2019) 1943–1955, https://doi.org/10.1021/acscatal.8b04289.
[31] J.S. Kim, G.G. Choi, Pyrolysis of Lignocellulosic Biomass for Biochemical Production, Elsevier B.V, 2018, https://doi.org/10.1016/B978-0-444-63992-9.00011-2.
[32] J. Yu, N. Paterson, J. Blamey, M. Millan, Cellulose, xylan and lignin interactions during pyrolysis of lignocellulosic biomass, Fuel. 191 (2017) 140–149, https://doi.org/10.1016/j.fuel.2016.11.057.
[33] Y. Wei, D. Wu, D. Wei, Y. Zhao, J. Wu, X. Xie, R. Zhang, Z. Wei, Improved lignocellulose-degrading performance during straw composting from diverse sources with actinomycetes inoculation by regulating the key enzyme activities, Bioresour. Technol. 271 (2019) 66–74, https://doi.org/10.1016/j.biortech.2018.09.081.
[34] D. Nowakowski, Biomass and Ash Characteristics and Analyses (ABC-Salt D3.2), 2019.
[35] P.R. Patwardhan, J.A. Satrio, R.C. Brown, B.H. Shanks, Influence of inorganic salts on the primary pyrolysis products of cellulose, Bioresour. Technol. 101 (2010) 4646–4655, https://doi.org/10.1016/j.biortech.2010.01.112.
[36] J. He, Y. Yang, C. Zou, Q. Gao, H. Hu, K. Xu, X. Li, H. Yao, Investigation of the reaction mechanism regarding thermal treatment of biomass using molten salts: a kinetic study of small molecule gases formation, J. Environ. Chem. Eng. 11 (2023) 1–10, https://doi.org/10.1016/j.jece.2022.109094.
[37] G. Bai, X. Wen, L. Niu, Recent Developments in Amorphous Alloy Catalysts for Hydrogenation, Elsevier Inc., 2016, https://doi.org/10.1016/b978-0-12-409547-2.11034-0.
[38] F. Morteo-Flores, A. Roldan, Mechanisms and trends of guaiacol hydrodeoxygenation on transition metal catalysts, Front. Catal. 2 (2022) 1–12, https://doi.org/10.3389/fctls.2022.861364.
[39] R. Shu, Y. Xu, L. Ma, Q. Zhang, P. Chen, T. Wang, Synergistic effects of highly active Ni and acid site on the hydrodeoxygenation of syringol, Catal. Commun. 91 (2017) 1–5, https://doi.org/10.1016/j.catcom.2016.12.006.
[40] K. Venkatesan, J.V.J. Krishna, S. Anjana, P. Selvam, R. Vinu, Hydrodeoxygenation kinetics of syringol, guaiacol and phenol over H-ZSM-5, Catal. Commun. 148 (2021), https://doi.org/10.1016/j.catcom.2020.106164.
[41] K. Yan, G. Wu, T. Lafleur, C. Jarvis, Production, properties and catalytic hydrogenation of furfural to fuel additives and value-added chemicals, Renew. Sust. Energ. Rev. 38 (2014) 663–676, https://doi.org/10.1016/j.rser.2014.07.003.
[42] T. Matamba, A. Tahmasebi, S.K. Rish, J. Yu, Understanding the enhanced production of poly-aromatic hydrocarbons during the pyrolysis of lignocellulosic biomass components under pressurized entrained-flow conditions, Fuel Process. Technol. 213 (2021), https://doi.org/10.1016/j.fuproc.2020.106645.
[43] P.R. Patwardhan, R.C. Brown, B.H. Shanks, Understanding the fast pyrolysis of lignin, ChemSusChem. 4 (2011) 1629–1636, https://doi.org/10.1002/cssc.201100133.
[44] L. Li, R. Van De Vijver, A. Eschenbacher, F.H. Vermeire, K.M. Van Geem, Experimental and kinetic modeling study on the gas-phase pyrolysis of hydroxycinnamaldehyde model compounds, Energy Fuel 36 (2022) 12031–12045, https://doi.org/10.1021/acs.energyfuels.2c02042.
[45] X. Zhang, S. Xu, Q. Li, G. Zhou, H. Xia, Recent advances in the conversion of furfural into bio-chemicals through chemo- and bio-catalysis, RSC Adv. 11 (2021) 27042–27058, https://doi.org/10.1039/d1ra04633k.
[46] S. Chen, R. Wojcieszak, F. Dumeignil, E. Marceau, S. Royer, How catalysts and experimental conditions determine the selective hydroconversion of furfural and 5-

hydroxymethylfurfural, Chem. Rev. 118 (2018) 11023–11117, https://doi.org/10.1021/acs.chemrev.8b00134.

[47] A. Osatiashtiani, J. Zhang, S.D. Stefanidis, X. Zhang, A.V. Bridgwater, The mechanism for catalytic fast pyrolysis of levoglucosan, furfural and furan over HZSM-5: an experimental and theoretical investigation, Fuel. 328 (2022), 125279, https://doi.org/10.1016/j.fuel.2022.125279.

[48] Q. Lu, Z. Wang, C.Q. Dong, Z.F. Zhang, Y. Zhang, Y.P. Yang, X.F. Zhu, Selective fast pyrolysis of biomass impregnated with ZnCl2: Furfural production together with acetic acid and activated carbon as by-products, J. Anal. Appl. Pyrolysis 91 (2011) 273–279, https://doi.org/10.1016/j.jaap.2011.03.002.